Journal of Intelligent & Robotic Systems (2021) 102: 76
https://doi.org/10.1007/s10846-021-01423-0

REGULAR PAPER

Biomechanical Assessment of Adapting Trajectory and Human-Robot Interaction Stiffness in Impedance-Controlled Ankle Orthosis

João M. Lopes [1] · Joana Figueiredo [1] · Cristiana Pinheiro [1] · Luís P. Reis [2] · Cristina P. Santos [1]

Received: 16 August 2020 / Accepted: 21 May 2021 / Published online: 8 July 2021

Abstract
Gait disabilities empowered intensive research on the field of human-robot interaction to promote effective gait rehabilitation. Assist-as-needed strategies are becoming prominent, appealing to the users' participation in their rehabilitation therapy. This study proposes and assesses the biomechanical effects of an adaptive impedance control strategy that innovatively allows adaptability in interaction-based stiffness and gait trajectory towards a fully assist-as-needed therapy. By modulating the interaction-based stiffness per gait phase, we hypothesize that the strategy appeals to a symbiotic human-orthotic cooperation, augmenting the user's muscular activity. The interaction stiffness was estimated by modelling the human-orthosis interaction torque vs angle curve with a linear regression model. The strategy also allows for real-time trajectory adaptations at different gait phases to fulfil the users' needs. The biomechanical assessment of the impedance-controlled ankle orthosis involved eight healthy volunteers walking at 1.0 and 1.6 km/h. The results revealed a stronger muscular activation regarding the non-assisted leg for the *gastrocnemius lateralis* (increment ratio ≥ 1.0 for both gait speeds) and for the *tibialis anterior* muscle (increment ratio ≥ 1.0 for 1.6 km/h). The strategy guided users successfully on a healthy gait pattern while allowing deviations (median error $< 5.0°$) given the users' intention weighted by interaction stiffness. Findings showed the relevance for adapting gait trajectory as users prefer higher trajectories as the speed increases. No significant temporal variations or neither knee angular compensations were observed (p value ≥ 0.11). Overall results support that this strategy may be applied for intensity-adapted gait training, allowing different human-robot compliant levels.

Keywords Adaptive assistive strategies · Impedance control · Human-orthosis interaction · Locomotion and actuation systems · Robotic rehabilitation

1 Introduction

Dysfunctional gait is a common disability among European countries. It is estimated that more than 5 million European persons suffer from a gait disability and dependent on a wheelchair [1]. Gait disabilities are caused by the natural process of aging, but also due to the increased incidence of cardiovascular and neurological disorders on the World's population [2]. Stroke, for instance, is the third cause of disability worldwide. Patients with impaired gait may require a complete, assist-as-needed, and patient-oriented rehabilitation to empower their long-term functional motor recovery. This triggered intensive biomedical research in the use of robotic devices towards gait rehabilitation.

To date, numerous orthotic devices have been proposed to provide or restore the locomotion in persons with motor disabilities. Some examples are the multi-segment devices such as ATLAS [3], HAL [4], ReWalk [5], Vanderbilt [6], MINA [7], Lokomat [8], and LOPES [9], while other studies, namely Ferris et al. [10], Herr et al. [11] and Kao et al. [12], proposed single-segment orthoses.

Most of the current devices assist the end-user considering a predefined gait trajectory, where a position control is systematically performed based on the periodicity of the gait. It is an important and suitable strategy for the first therapy's stages since it delivers a periodic movement to the articulation, contributing to decrease the muscle atrophy and regain the motor functionalities [2]. The orthosis trajectory is a mimic from the

✉ João M. Lopes
a74982@alunos.uminho.pt

[1] Centre for MicroElectroMechanical Systems (CMEMS), University of Minho, 4800-058 Guimarães, Portugal

[2] Artificial Intelligence and Computer Science Laboratory (LIACC), University of Porto, 4200-465 Porto, Portugal

healthy gait pattern, recorded with standard motion equipment from a set of healthy subjects. However, this gait trajectory may not be the most adequate for each patient, attending to his/her anthropometry and motor and physiological needs. Thus, the need for an effective and personalized rehabilitation arose considering patient-oriented gait trajectories. For instance, the Lokomat allows angle trajectory modifications in time, range-of-motion, and offset [8]. LOPES' exoskeleton also allows for gait trajectory modifications according to the gait speed. However, new directions highlight the relevance for adapting trajectories considering specific gait phases to improve the user's physiological coordination and recover the natural gait pattern described by Winter [13] and Perry [14]. To the best knowledge of the authors, such adaptability still needs to be addressed.

As the patient progresses in the rehabilitation, the therapy should be gradually adapted. The orthosis should provide intensity-adapted exercises, passing from an active mode of assistance, where it imposes a patient-guided trajectory, to a more passive mode, where the patient can freely interact with the assistive device [2, 15]. This approaches a multi-functional gait training that can be accomplished with assist-as-needed (AAN) control strategies [15]. With a therapy sustained in human-robot cooperation, the patient is encouraged to apply effort in the therapy and actively participate, activating their muscles and, thus, enhancing their functional motor ability [9, 16]. Some authors have presented adaptive impedance control algorithms to solve this challenge, adapting the device's assistance considering the patients' active torque (muscular torque estimation). Example includes the Lokomat [8], LOPES' robot [9], and the orthosis presented by Hussain et al. [17]. The variation of impedance parameters, namely stiffness, results in different forces acting at the joint, allowing a compliant or stiffer behaviour [8, 9, 17]. Lokomat exoskeleton implements a first-order impedance model in which the reference torque acting at the joint is modulated considering linear elastic (K) and linear viscous (B) coefficients [8]. This reference torque is then compared to the joint's moment, generated by the user's muscles. The therapist may decide how much the robot supports the user's movement. The authors reported angular deviations from the reference trajectory when the robot increased its compliance, which are caused by the muscular effort of the patient [8]. LOPES is a bilateral exoskeleton and impedance controlled by Bowden-cable-driven series-elastic actuator [9]. This robot promotes two modes of assistance, the robot-in-charge and the patient-in-charge, by modulating the subject-specific percentage of maximum stiffness allowed by the exoskeleton. The authors reported a closer approximation to the reference trajectory and a reduction in the movement's variability when high levels of impedance are set. The same principles of Lokomat and LOPES exoskeletons were implemented into a pneumatic orthosis in [17]. The authors reported the increased users' participation when low assistance is given by the robot [17]. In [18, 19], a first-order impedance model was presented by modulating the stiffness and damping parameters of an active hip-knee-ankle exoskeleton. The authors used an observer-based approach associated with a Kalman filter to estimate the user's musculoskeletal torque. In [18], the stiffness and damping parameters were estimated using the least square method and, in [19], the authors proposed a model predictive control to estimate stiffness. The authors reported that the proposed strategy was effective in setting the level of robot assistance. In [20, 21], an assistive-resistive approach was proposed by applying an adaptive first-order impedance control to an ankle orthosis. The authors found that the adaptive assistance allowed a more kinematic variability. Nonetheless, these studies focus on adapting the joint's stiffness instead of the interaction-based stiffness, which directly allows a therapy sustained in human-robot cooperation. Further, the adaptation has not been accomplished at different gait phases, which could be relevant since the users may interact differently and require variable assistance within the gait cycle. In our preliminary study [22], we evaluated the human-orthosis interaction stiffness all over the gait cycle and for different gait speeds. However, the biomechanical effects of changing the interaction stiffness per gait phase were not assessed.

This study includes two main goals. First, it presents a novel approach of an AAN and adaptive impedance control that gathers the potentialities of adaptive human-orthosis interaction stiffness with the relevance of adapting gait trajectories per gait phase. The strategy innovatively allows the gait trajectory modification in real-time at four main phases of dorsiflexion and plantarflexion through a user-friendly mobile app that attends to the clinician expertise, extending our previous study [22]. The interaction-based stiffness is estimated per gait phase and speed through a linear fit to the human-orthosis interaction torque vs angle curve [22]. This strategy advances current robotics-based gait rehabilitation beyond the state-of-the-art, as follows: i) the adaptability of human-orthosis interaction stiffness across different gait phases and speeds, advancing [8, 9, 17–21], that enables a multi-functional gait training by modulating the orthosis' compliance with the user as needed and encourage the users to actively participate in their recovery process; and ii) the adaptability of gait trajectory considering different gait phases, extending [22] and advancing [8, 17–21], which tackles current challenges in patient-oriented strategies to improve the user's motor coordination and it allows to address the rehabilitation of diverse gait pathologies. Table 1 presents the comparison of the proposed study regarding state-of-the-art.

We hypothesize that this strategy, by adapting the trajectory and human-robot interaction stiffness, encourages the users to apply more physical effort; thus, enhancing their muscular activity in the assisted leg. In this sense, our second goal advances by assessing the biomechanical effects of the

proposed strategy on the muscular variation under single and combined parameter's adaptation (i.e., interaction-based stiffness and trajectory), extending our previous study [22] and state-of-the-art [8, 9, 17–21], as stated in Table 1. Additionally, we also evaluated the variation in temporal, kinematic and kinetic parameters for the assisted leg. From the results with eight healthy volunteers walking with ankle robotic orthosis, we verified the suitability of this approach to improve the human-robot interaction by appealing to the active participation of the user on his/her rehabilitation therapy. Moreover, the effect of compliance/resistance promoted an active muscular activity. The real-time trajectory adaptation was relevant to consider the users' will.

2 Methodology

Through a literature analysis, we acknowledge the need for a user-oriented assistive strategy that better fulfils the user's necessities and encourages them to actively participate in therapy [2, 16]. In this work, we present an AAN impedance strategy that allows the angle's trajectory modification and the interaction stiffness adaptation in real-time for different phases of the gait cycle. With this strategy, the clinician may create user-oriented and intensity-adapted exercises considering the user's disability towards effective gait rehabilitation. This section presents the methodology, specifying the wearable orthosis and the multi-functional adaptive assistive strategy.

2.1 Robotic Ankle Orthosis

This study involved an electrically actuated wearable ankle-foot orthotic device (PAFO) from the H2-Exoskeleton (Technaid S.L., Spain). The device provides one degree-of-freedom in the sagittal plane using a flat brushless DC motor coupled to a gear box. It is hierarchically controlled, diving the control strategy into high-, mid- and low-level [23].

The system is fed by a 24 V LiFePO4 DC battery, making it completely wearable and suitable for clinical usage. The orthosis contains an embedded strain gauge placed on a Wheatstone bridge to monitor the human-orthosis interaction torque and a potentiometer close to the ankle's articulation to measure the angle trajectory in the sagittal plane. The system is controlled by a user-friendly mobile app, which allows the system's and therapy's settings easily and intuitively.

2.2 Adaptive Impedance Control

The adaptive impedance control aims to provide cooperation and interaction between the user and the assistive device. Instead of imposing a pre-defined gait trajectory, the orthosis allows for deviations in the angle trajectory that depends on the user's participation [8, 17]. Endowing orthoses with an impedance control may benefit the users' recovery since they are encouraged to actively interact with the assistive device, i.e., a strategy sustained in human-robot cooperation. This feeling of self-contribution in the rehabilitation can be beneficial to improve the user's motor learning and muscular tonus [16]. Figure 1 presents the block diagram of the impedance control implemented in this work.

The high-level, running in a Raspberry Pi 3 (Raspberry Pi Foundation, UK) at 100 Hz, is responsible for the central control, generating the adapted reference trajectory (θ_{REF}) and setting the interaction stiffness values per gait phases (K_{INT}) according to the settings specified in a mobile application by the clinician. The reference trajectory and the interaction stiffness values are then sent to the mid-level control.

Table 1 Comparison of the proposed study with the state-of-art

Study	Type of actuator	Targeted joint	Adapted parameter(s)	Trajectory adaptation(s)	Kinematic & kinetic study	Physiological study
[8]	Electric	HK	Robot's stiffness and damping	Trajectory as a whole	+	–
[9]	Bowden-cable-driven series-elastic	HK	Robot's stiffness	Trajectory as a whole	+	+ (Clinical scales)
[17]	Pneumatic	HK	Robot's stiffness	Trajectory as a whole	+	–
[18]	–	HKA (simulation)	Joint's stiffness and damping	–	+	–
[19]	Series elastic	K	Robot's stiffness	–	+	–
[20, 21]	Electric	A	Robot's stiffness	Programmable	+	–
Ours	Electric	A	Human-robot interaction stiffness per gait phases and speeds	Adapted per gait phases and as a whole	+	+ (EMG)

A – ankle; HKA – hip, knee, and ankle; HK – hip and knee; K – knee

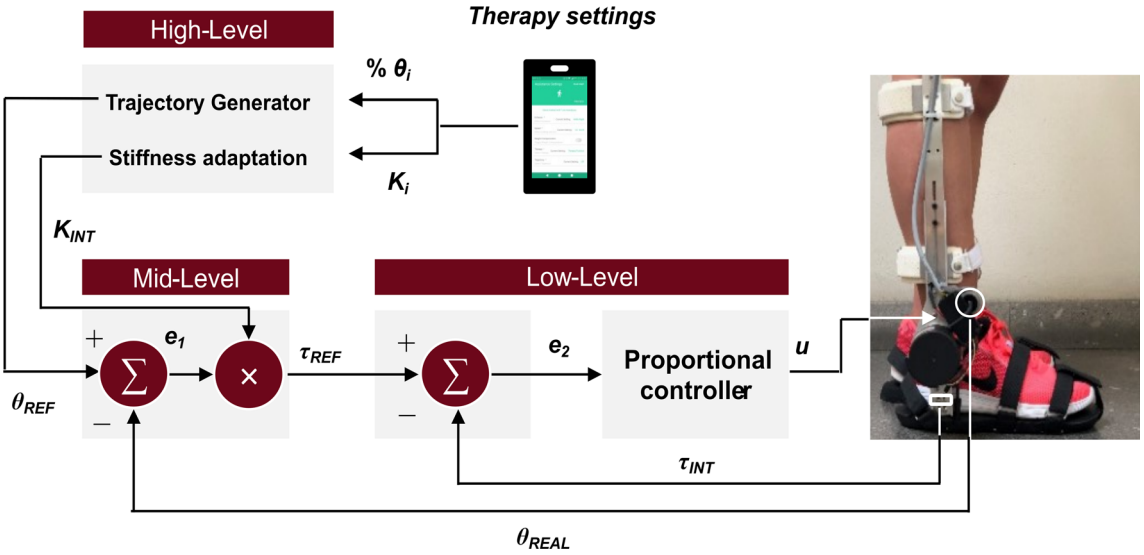

Fig. 1 Block diagram of the proposed adaptive impedance control: K_i corresponds to the values of interaction stiffness per gait phase defined by the clinician; $\%\theta_i$ corresponds to the percentual factors of each gait phase defined by the clinician; θ_{REF} corresponds to the orthosis' reference trajectory; θ_{REAL} corresponds to the real trajectory; K_{INT} corresponds to the stiffness values per gait phase to be sent to the mid-level control; e_1 corresponds to the error between the reference and the real trajectory; τ_{REF} corresponds to the adaptive reference torque; e_2 corresponds to the error between the adaptive reference torque and the human-orthosis interaction torque (τ_{INT}); and u corresponds to the controller's command

The mid-level control runs at 100 Hz in an STM32F4-Discovery (STMicroelectronics, Switzerland). It is responsible for scaling the reference trajectory considering each admitted speed (between 0.5 and 1.6 km/h) according to (1) that sets the Number of Control Loops (NCL) for each value of the reference trajectory generated in the high-level.

$$NCL = -34.62 \times Gait\ Speed + 107.31 \quad (1)$$

Additionally, this control level implements the zero-order impedance control law [24]. It calculates the error between the reference trajectory (θ_{REF}) and the real ankle trajectory (θ_{REAL}) and multiplies this error by the interaction stiffness (K_{INT}), as presented in (2), to estimate the reference interaction torque (τ_{REF}).

$$\tau_{REF} = K_{INT}\ (\theta_{REF} - \theta_{REAL}) = K_{INT}\ e_1 \quad (2)$$

As an impedance strategy, the goal is to provide more or less freedom to the patients' movement considering, respectively, low and high levels of interaction stiffness. With high values of interaction stiffness, the orthosis is more rigid and imposes more the reference trajectory. By controlling the values of interaction stiffness, the torque that the orthosis provides is also controlled, varying the patients' interaction and effort to keep the desired gait pattern. As an AAN assistive strategy, it assists the patient only where and when needed. In this work, we considered the deviation from the reference trajectory as an assist-as-needed indicator.

Based on this strategy, the reference torque is zero (or near zero): a) if the user is following the orthosis' reference trajectory which indicates the user does not need assistance. In this case, the orthosis does not provide any torque assistance and responds only to the user's interaction; or b) if the interaction stiffness is set to low levels, encouraging the users to actively participate, enhancing their recovery by applying more effort and activating their muscles. This situation is considered similar to the one in which the orthosis acts as a passive device without providing any assistance. On the other hand, if the user is not following the orthosis' reference correctly, the reference torque is different from zero. Depending on the magnitude of the error, the corrective torque is generated and sent to the low-level control where it is compared against the human-orthosis interaction torque (τ_{INT}). In this work, we acknowledge the interaction torque as a measure of the user's participation.

The low-level control, that runs in a STM32F4-Discovery (STMicroelectronics, Switzerland) at 1000 Hz, consists of a proportional controller. It is responsible for generating an adequate response (u) regarding the error between the reference torque and the human-orthosis interaction torque (e_2) – see Fig. 1. The proportional controller was tuned according to the Ziegler-Nichols method with a subset of subjects in the loop [25], while considering a trade-off between system's stability and the delay to avoid oscillations in the real environment. We used the proportional gain as $K_p = 120$ [22].

2.3 Adaptive Gait Trajectories

As a fully adaptable assistive strategy, the AAN impedance control allows for real-time modification of the reference trajectory using the user-friendly mobile app. The reference

trajectory was generated through a cohort of healthy participants and follows the principles described by Perry [14]. From this reference trajectory, it is possible to produce numerous reference trajectories in real-time while maintaining the integrity and continuity of the natural gait pattern. For that, we developed an algorithm, integrated into the PAFO's high-level control, that considers the main phases of the gait cycle to create enough number of reference trajectories to fulfil the user's necessities. These modifications may be performed considering the dorsiflexion and plantarflexion phases of the gait cycle [14], as shown in Fig. 2. The adjustment may be customized to each phase or considering the entire trajectory.

We considered the neutral angle (zero degrees) as the basis of our trajectory adaptation to ensure the continuity and adaptability effect of the entire gait trajectory. In this algorithm, it is assigned a percentual change factor between 1% and 100%, considering a resolution of 1%, for each phase of dorsiflexion and plantarflexion to build a kernel with equal size to the reference trajectory, responsible for the real-time modifications. Multiplying each i-th value of kernel by the corresponding value of the reference trajectory will create the user-specific trajectory. We considered a default of 60% of a healthy trajectory as the user must accomplish since a value beneath this threshold generates a non-functional gait training. Nevertheless, this value can be reassigned if needed. With this approach, it is possible to create different trajectories tailored to the user's level of disability by varying the healthy trajectory through a ratio that varies from 60% to 100%. This ratio may be customized to each gait phase or to be similar to the entire gait cycle. Figure 2 displays examples of possible generated gait trajectories that serve as the reference for the low-level controller.

2.4 Adaptive Human-Orthosis Interaction Stiffness

The rotational stiffness of the joint, usually known as mechanical stiffness [8], is considered the ratio between a moment M, induced by a force F, and the rotation θ. Considering M the torque that is actuating at the ankle joint, and θ the resulting angle, the ratio gives the stiffness of the joint. However, in our work, we do not use this. We applied this ratio to the human-orthosis interaction torque measured by the strain gauges. We considered the human-orthosis interaction torque as a motion and participation indicator to change the orthosis' compliance. Its magnitude represents the user's participation, while the signal's monotony represents the user's motion. The force

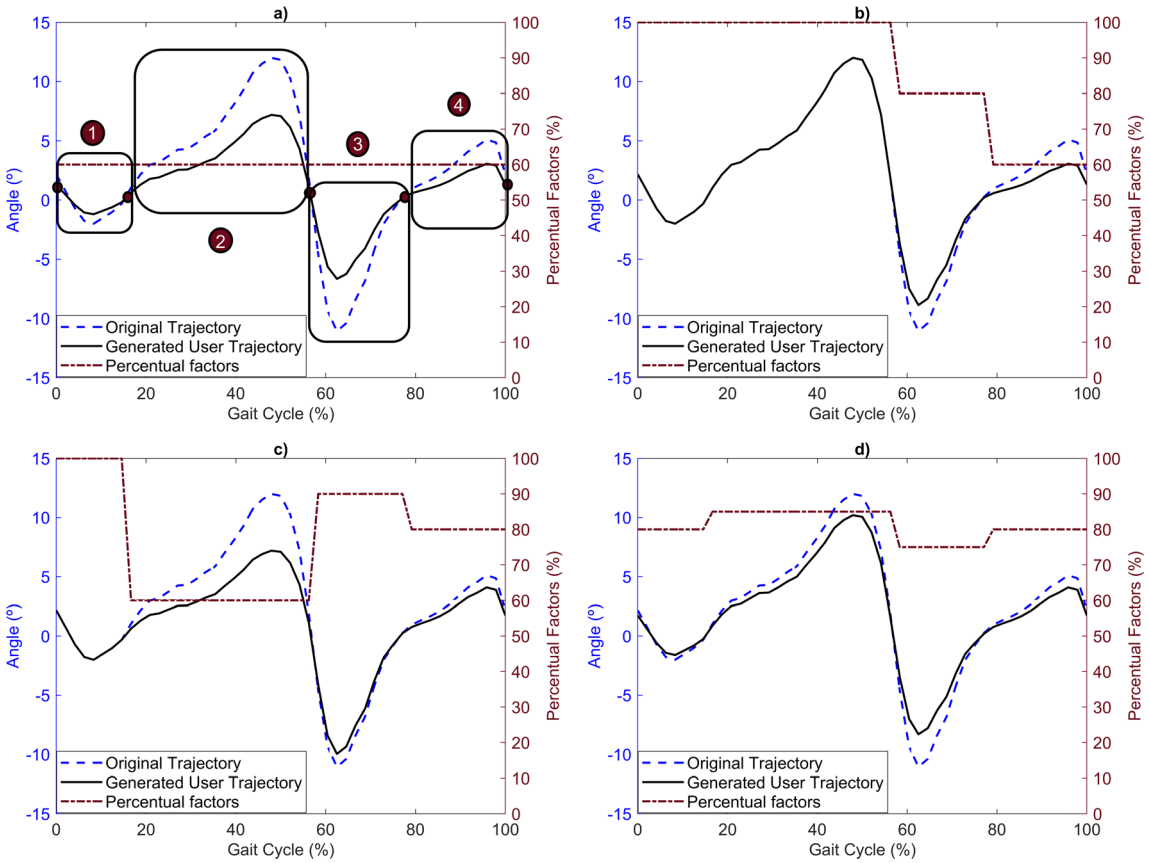

Fig. 2 Possible generated gait reference trajectories for the low-level proportional controller, considering the main phases of dorsiflexion (2 and 4) and plantarflexion (1 and 3) and the percentual ratios of: **a**) 60% for all phases, **b**) 100% - 100% - 80% - 60%, **c**) 100% - 60% - 90% - 80%, and **d**) 80% - 85% - 75% - 80%

the user applies to perform the intended movement induces a deformation into the strain gauges, translating the user's participation and motion into a measurable variable.

By calculating the ratio between the human-orthosis interaction torque and the real angle, we derived a virtual stiffness that we called the "human-orthosis interaction stiffness". The particularity of our approach is that we estimated this parameter considering different phases of the gait cycle and gait speeds, allowing to infer in which phases the user participates more (i.e., a higher magnitude is expected from the interaction torque) and if this participation differs considering the gait speed. By modulating the interaction stiffness for different gait phases, the orthosis' contribution can be diminished in those phases in which the user is capable of, giving place to the user's contribution, and augmented in those phases where the users require assistance.

The interaction stiffness was estimated by linear approximation to the human-orthosis interaction torque vs angle curve, following the least-square method [26]. This method evaluates the best approximation that produces minimal deviations regarding the target signal. We set the interaction stiffness as the slope of the best curve that approximates the human-orthosis interaction torque vs angle trajectory, K_{INT}, considering (3).

$$K_{INT} = \frac{n\sum x_i y_i - \sum x_i \sum y_i}{n\sum x_i^2 - (\sum x_i)^2} \tag{3}$$

The interaction stiffness was estimated from an empiric analysis involving healthy participants, as presented in [22]. The values were normalized by body mass and normalized between 0 and 1 to allow a general analysis among participants, avoiding extreme values. By analysing the human-orthosis interaction torque vs angle curve, we verified the need to adapt the interaction stiffness for six different phases of the gait cycle, mainly during the movements of foot's dorsiflexion and plantarflexion. The gait phases, illustrated in Fig. 3, were automatically segmented by a finite state machine using the angular velocity recorded by an inertial measurement unit (IMU) placed on the foot, as presented in our previous study [22] and validated in [27] through controlled and real-life walking situations.

Table 2 presents the default values discriminated per gait speed that we found with our previous study [22]. The interaction stiffness was estimated in offline for these gait phases. However, these values may be adapted in real-time by qualified clinical staff to fulfil the user's needs. If the user is progressing in the therapy, the clinician can gradually decrease the interaction stiffness and appeal to the users' participation. The high-level control is responsible for setting the interaction stiffness values considering the gait speed.

2.5 Safety

We implemented safety measures in our orthosis to ensure the users' safety. The orthosis ROM was limited to 40° (between

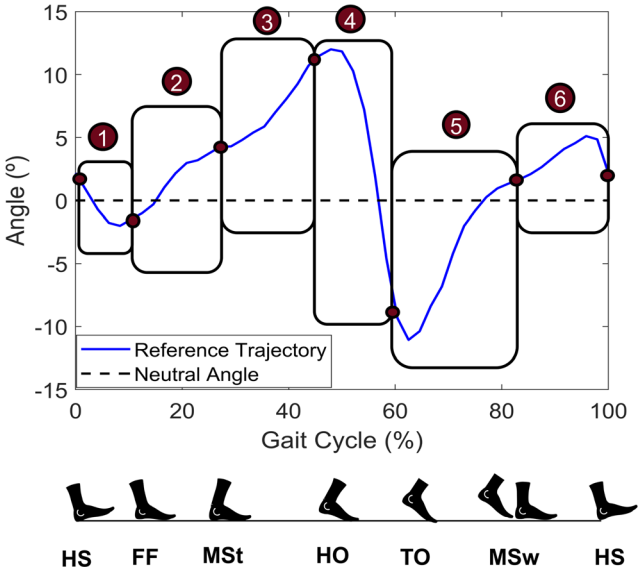

Fig. 3 Phases of the gait cycle for which the human-orthosis interaction stiffness was estimated: 1) Heel-strike (HS) → Flat foot (FF); 2) FF → Mid-Stance (MSw); 3) MSw → Heel-off (HO); 4) HO → Toe-off (TO); 5) TO → Mid-Swing (MSw); and 6) MSw → HS

20° of plantarflexion and 20° of dorsiflexion) to not allow a non-physiological gait pattern to the end-user. All trajectory's modifications were applied to the next gait cycle to the one where they were set, maintaining the pattern's integrity and not produce sudden changes while walking. Moreover, a saturator was added to the proportional controller to avoid instabilities that compromise the user's confidence and safety when using the orthosis. Magnitude of control commands (u, Fig. 1) was set to the interval [−2500, 2500], i.e., to the maximum values of the orthosis' pulse-width modulation. The values of interaction stiffness were normalized to [0, 1].

3 Experimental Validation

To address the second goal of this study, we performed an experimental study, validating the novel proposed adaptive impedance strategy and evaluating the variation in biomechanical metrics along with trajectory and interaction stiffness adaptation. The study was conducted in the University of Minho under the ethical procedures of the Ethics Committee in Life and Health Sciences (CEICVS 006/2020), following the Helsinki Declaration and the Oviedo Convention. All subjects accepted to participate voluntarily and gave their informed consent to be part of the study.

3.1 Participants

Eight able-bodied subjects (six males and two females, body mass: 68.5 ± 12.6 kg, height: 172 ± 11.8 cm, age: 25.5 ± 1.51 years) were recruited from the Biomedical Robotic

Table 2 Interaction stiffness normalized by gait phase, stance and swing, single (gray cell) and double support (while cell)

Gait speed (km/h)	Gait Phases	Normalized Interaction Stiffness		
		Interaction stiffness	*Stance vs Swing*	*Single vs Double Support*
1.0	HS → FF	0.64 ± 0.38	0.51 ± 0.28	0.64 ± 0.38
	FF → MSt	0.48 ± 0.29		0.31 ± 0.24
	MSt → HO	0.14 ± 0.05		
	HO → TO	**0.79 ± 0.17**		0.79 ± 0.17
	TO → MSw	0.74 ± 0.19	0.78 ± 0.05	0.78 ± 0.05
	MSw → HS	0.82 ± 0.25		
1.3	HS → FF	0.25 ± 0.14	0.36 ± 0.33	0.25 ± 0.14
	FF → MSt	0.29 ± 0.13		0.18 ± 0.16
	MSt → HO	0.07 ± 0.04		
	HO → TO	**0.84 ± 0.23**		0.84 ± 0.23
	TO → MSw	0.58 ± 0.33	0.56 ± 0.04	0.56 ± 0.04
	MSw → HS	0.53 ± 0.28		
1.6	HS → FF	0.52 ± 0.35	0.57 ± 0.28	0.52 ± 0.35
	FF → MSt	0.84 ± 0.13		0.52 ± 0.46
	MSt → HO	0.19 ± 0.05		
	HO → TO	**0.71 ± 0.41**		0.71 ± 0.41
	TO → MSw	0.49 ± 0.05	0.47 ± 0.03	0.47 ± 0.03
	MSw → HS	0.45 ± 0.13		

Devices Laboratory of the Centre for Microelectromechanical Systems (University of Minho) to participate in the experimental evaluation. A list of inclusion and exclusion criteria was outlined. All subjects that presented healthy locomotion and a total balance of posture, had 18 or more years, a body mass within 45 and 90 kg, and a height within 150 and 190 cm, were accepted to participate in the study. The anthropometry criteria were imposed due to the orthosis' mechanical system. The required anthropometric data, presented in Table 3, were collected before the experimental sessions.

3.2 Instrumentation

The participants were instructed to wear shorts and a standard type of sports shoes. The participants were instrumented with the wireless motion tracker system MTw Awinda (Xsens Technologies B.V., Enschede, The Netherlands, validated in [28, 29]), wearing IMUs on the feet, shanks, thighs, and waist. The IMUs were placed on the lateral side of each segment and secured with a strap, as illustrated in Fig. 4. The participants were also instrumented with wireless EMG surface electrodes from the Trigno™ Avanti Platform (Delsys, Massachusetts, USA, validated in [29]) to measure the muscular activity of the *tibialis anterior* (TA) and *gastrocnemius lateralis* (GL) muscles of both right and left legs. The participant's skin was cleaned with alcohol (70%) to remove dead skin residues that may interfere with the measurement. The sensors were attached to the skin with double-sided tape according to the Surface ElectroMyoGraphy for the Non-Invasive Assessment of Muscles (SENIAM) recommendations [30]. To avoid sensor's disconnection from the skin, each sensor was fixed with a strap.

Table 3 Participant's anthropometric data required for the experimental procedure

Participant ID	Gender (M/F)	Body mass (kg)	Height (cm)	Age (years)
1	F	52	162	27
2	M	73	185	28
3	F	50	150	24
4	M	62	175	25
5	M	76	182	26
6	M	73	182	26
7	M	86	170	24
8	M	76	170	24

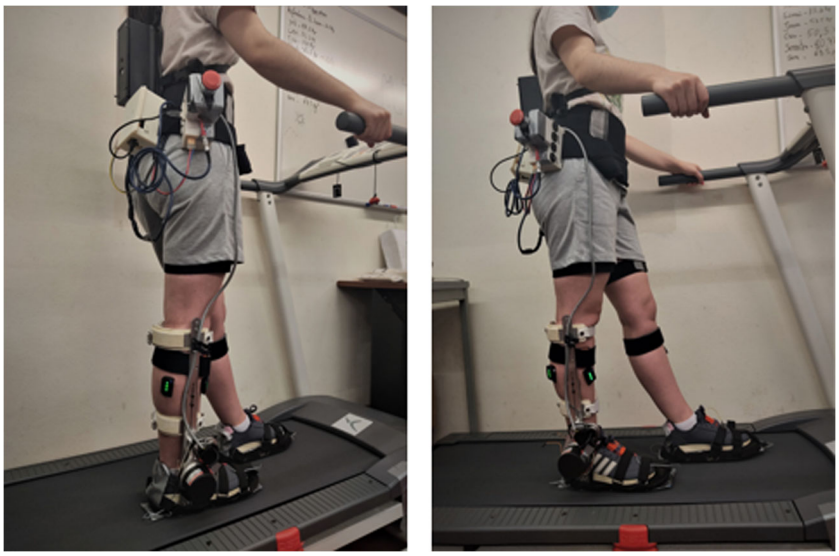

Fig. 4 Experimental setup for the adaptive impedance control validation. The participants were instrumented with the orthosis on the right leg, two EMG surface electrodes in each leg placed on the *tibialis anterior* and *gastrocnemius lateralis* muscles, and with IMUs on both feet, shanks, thighs, and hip

After the placement of the inertial and EMG sensors, the participants were instrumented with the ankle-foot robotic orthosis in the lateral side of the right leg, as illustrated on Fig. 4. An insole with the same width as that in the orthosis was instrumented on the left leg. Each insole was instrumented with two force sensitive resistor (FSR), one on the heel and another on the toe.

3.3 Experimental Protocol

Prior to the experimental acquisition and the orthosis placement, the anthropometric data required for the MVN software (height and foot length) was measured. Then, we calibrated the MVN BIOMECH in N-pose, following the MVN software guidelines (Xsens Technologies B.V., Enschede, The Netherlands).

After the successful placement of the EMG sensors, the participants performed three maximum voluntary contractions (MVCs) for each muscle to normalize the EMG data. The participants sat in a fixed chair and place each foot (one at a time) on another chair on the front with the knee slightly bent. With an assistant holding the participant's foot, the participant was instructed to perform the plantarflexion movement to measure the TA activation, and the dorsiflexion movement to measure the GL activation.

Subsequently, the subjects were instructed to walk on a treadmill at 1.0 and 1.6 km/h for three continuous trials of 10 min with a rest interval of 4 min. The participants experienced different conditions over the trials that were modified every 2 min using the mobile app. They were blind regarding the conditions they experienced. These conditions were sequentially performed to assess the effectiveness of the strategy to change in real-time the interaction stiffness and the orthosis' reference trajectory, and to assess the effects on the users' muscular activity and interaction. In the first two minutes of the trial, we set the orthosis' reference trajectory to 100% (the full reference trajectory, see Fig. 2) and the interaction stiffness values at their maximum admissible value ($K = 1$). In the following two minutes, we modified the interaction stiffness for the values that we found in our previous study [22], presented in Table 2 (note that these values can be real-time changed regarding the users' disability level and rehabilitation goal). Afterward, the interaction stiffness was maintained, and we changed the orthosis' reference trajectory, setting 100%, 100%, 80% and 60% for each of the four sub-phases. At the sixth minute, we performed a trajectory modification, setting 60% of the healthy pattern for the four sub-phases. Finally, in the last two minutes, we changed the interaction stiffness back to the maximum value, maintaining the orthosis' trajectory in 60% of the healthy pattern. Figure 5 illustrates the study design.

3.4 Data Acquisition

Data acquisition included: i) the ankle and knee joints angle for the assisted leg measured with the MTw Awinda; ii) the muscular activity of the TA and GL muscles using the 4-channel Trigno™ EMG sensors and Delsys acquisition software; iii) the orthosis' reference trajectory, real trajectory, human-orthosis interaction torque, reference interaction torque, and the FSRs data using the orthosis' integrated software. Data from the MTw Awinda and orthosis were acquired at 100 Hz, and the EMG data were measured at 2148 Hz. All data were timely synchronized.

Additionally, we collected the participants' perception regarding their experience with the orthotic device. A post-study questionnaire based on the standard system usability scale (SUS) [31, 32] was elaborated with nine questions, listed in Table 4. The questions were rated between 1 and 5, considering the scale "Strongly disagree", "Disagree", "Neutral",

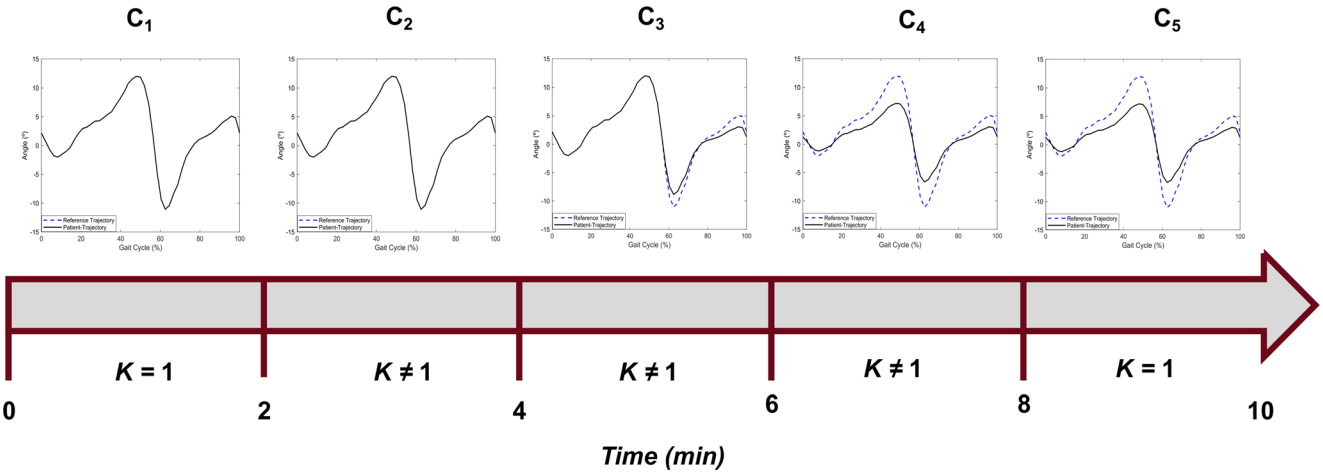

Fig. 5 Experimental protocol carried out for the strategy's validation with healthy subjects

"Agree", and "Strongly agree", except for the last question that was open-ended. The first four questions were more generic questions about the user's perception regarding the experimental procedure. From the fifth question, the participants were instructed to answer only and only if they answered positively to the fourth question.

3.5 Data Processing

All quantitative data was divided between conditions and segmented into gait cycles considering the heel-strike event. We averaged the gait cycles to each condition to obtain the mean gait cycle. The FSR data were also used to calculate the temporal parameters, namely the stance time, swing time, step time, and stride time. From the kinematic data, we calculated the maximum, minimum, and the trajectory's range-of-motion (ROM) for both ankle and knee joints. The root-mean-square error (RMSE) between the orthosis' reference trajectory and the real trajectory, and the control's delay were also determined per condition and gait speed.

EMG data was processed as follows. Data were rectified, and the EMG envelope was calculated following the root-mean-square (RMS) technique using a window size of 125 ms with an overlap of 62.5 ms. Then, we normalized the envelope considering the MVC measured for each muscle of both assisted and non-assisted lower limbs. Lastly, we determined the mean activation value.

To evaluate the biomechanical effects of changing the interaction stiffness and the orthosis' reference trajectory between conditions, we calculated the percentual variation by determining the increase/decrease relatively to the last experienced condition. A percentual value above 0% corresponds to an augmentation. Contrariwise, a percentual value underneath 0% corresponds to a decrease regarding the last condition. Data were disposed in a form of boxplots.

To assess the users' participation in the rehabilitation strategy, we computed the symmetry ratio using (4) considering the muscular activity of both assisted and non-assisted leg, $MA_{assisted}$ and $MA_{non\text{-}assisted}$, respectively.

$$Symmetry\ ratio = \frac{MA_{assisted}}{MA_{non-assisted}} \tag{4}$$

We performed a statistical analysis to assess statistically significant differences in the biomechanical metrics and control delay between consecutive conditions (i.e., between $C_1 \rightarrow C_2$, $C_2 \rightarrow C_3$, $C_3 \rightarrow C_4$, $C_4 \rightarrow C_5$) and gait speeds. Altogether, 101 statistical tests were conducted, according to the following steps: all data were tested for normality using the Shapiro-Wilk normality test. Considering this result, for parametric data, a two-tail and paired t-test was conducted. For non-parametric data, the counterpart two-tail Wilcoxon's test was performed. For all statistical tests, we set the level of confidence to 95% ($\alpha = 0.05$). The following null hypothesis

Table 4 Questionnaire that was present to the participants after the experimental procedure

Questions
1. I found the system easy to use.
2. I think the system guided me during the walk.
3. I felt confident using the system.
4. I was able to verify when the system changed its assistance/behaviour.
5. I felt these changes gave me more freedom to walk.
6. I felt these changes encouraged me to apply more effort during walking.
7. Upon the changes, I felt the system compliant.
8. Upon the changes, I felt the system offered me resistance.

(H_0) was assumed: *There is no statistically significant differences between consecutive conditions for the parameters in study (biomechanical metric or control delay).*

From the qualitative data, we computed the relative frequency, in percentage, of rates assigned to each question. The results are presented in a circular graph, illustrating the answers' distribution among categories (scales).

4 Results and Discussion

4.1 Adaptive Impedance Control Performance Analysis

Assist-as-needed strategies have shown to be prominent for robotics-based gait rehabilitation, enhancing human-robot cooperation. In this work, we present and validate an assist-as-needed zero-order impedance control strategy for an ankle-foot robotic orthosis. By modulating the human-orthosis interaction stiffness, that changes the reference torque of a proportional controller, the strategy can change the orthosis behaviour by passing from a more passive mode of assistance to a more active one considering the users' disability level. The novelty of our investigation conjugates the orthosis' assistance adaptation within sub-phases of the gait cycle with a meticulous trajectory adaptation that fulfils the user's needs. Both trajectory and stiffness adaptations were performed in real-time using a user-friendly mobile app.

Altogether, were analysed more than 8000 gait cycles of 45 successful trials considering both 1.0 and 1.6 km/h. Figure 6 displays the mean gait cycle for the real trajectory, the human-orthosis interaction torque, and the reference interaction torque considering the five conditions that each subject experienced.

By analysing Fig. 6, the results demonstrate the continuity of the modifications that were made. It is observable that the orthosis can guide the users during the walking procedure for all the five conditions that were tested. There is a similarity between the reference trajectory and the real ankle trajectory that is accomplished by a closer cooperation between the user and the orthotic device. During condition 1 (C_1), the interaction stiffness was set to the maximum admissible value ($K = 1$) and, thus, the orthosis acts more actively, assisting the end-user if his/her is not following the reference trajectory. From the results, we can see a lower variation on the real ankle trajectory that indicates that the orthosis is imposing more its reference trajectory, as it was expected to occur. Between the transition $C_1 \rightarrow C_2$, the interaction stiffness was modified according to the values of Table 2. The orthosis immediately gave more freedom to the end-user since a higher dispersion of the real ankle trajectory was observed. We can see, from the non-zero interaction torque of Fig. 6, that this strategy allowed for some deviations around the reference trajectory proportional to the user's active participation. During the transition $C_2 \rightarrow C_3$, the orthosis' reference trajectory was modified. This reference trajectory presented a lower value for the HO → TO phase (80% of the Fig. 2 – phase 3) and for the TO → HS phase (60% of the Fig. 2 – phase 4). From Fig. 6, we verified that the users successfully followed the orthosis reference trajectory, visible with the minimum of the real ankle trajectory that dropped considering the last condition (C_2). The same conclusion is observable for the transition $C_3 \rightarrow C_4$, in which the orthosis' reference trajectory was placed to 60% for all four sub-phases. The angular dispersion was, however, slightly higher in comparison with the last condition (C_3), highlighting the ability of this strategy to empower the users' participation when lower values of interaction stiffness are set. When the interaction stiffness returned to the maximum admissible value, the dispersion around the reference trajectory decreased significantly, more visible during the stance phase (HS → TO). This result was expected since the orthosis should impose more its reference trajectory.

Figure 6 also enhances the aptness of our adaptive impedance control as an AAN strategy. It is observable that the users follow more the orthosis' gait pattern during the stance phase, as the reference interaction torque values do not present high variations. In fact, the assistive torque is almost null, indicating that the user may need punctual assistance once and while but the similarity between the reference gait trajectory and the real one is accomplished with the active participation that users are performing. On the other hand, during the swing phase, the more critical phase for subjects [22], the orthosis' adaptive reference torque presents a higher variation given the higher error in angle's magnitude. This torque is more evident during the HO → TO phase given the higher angular variation that is observed in a short time. Despite the muscular activation that we observed under this phase for the *gastrocnemius lateralis* muscle, the users are still unable to reach the reference angle and, thus, the orthosis assists with a higher reference interaction torque. However, it should be noticed that this assistive torque is not intended to impose completely the orthosis' reference trajectory when $K = 1$, as it is visible in Fig. 6. It is intended to help the user reaching the healthy pattern, otherwise, it would cause an abrupt change on users' gait that could cause their destabilization.

Figure 7 shows the RMSE dispersion considering the five conditions that each user experienced for both gait speeds. Note that the human-orthosis delay was not accounted for the RMSE calculation.

Analysing Fig. 7, it is visible that the RMSE dispersion for both gait speeds is more pronounced for C_2, C_3, and C_4, in which the interaction stiffness is lower than 1 ($K \neq 1$). This error was accomplished by the higher angle dispersions of the real ankle trajectory visible on Fig. 6 for those conditions in which the orthosis is more compliant. It is also visible that the error regarding the reference trajectory is higher for 1.6 km/h

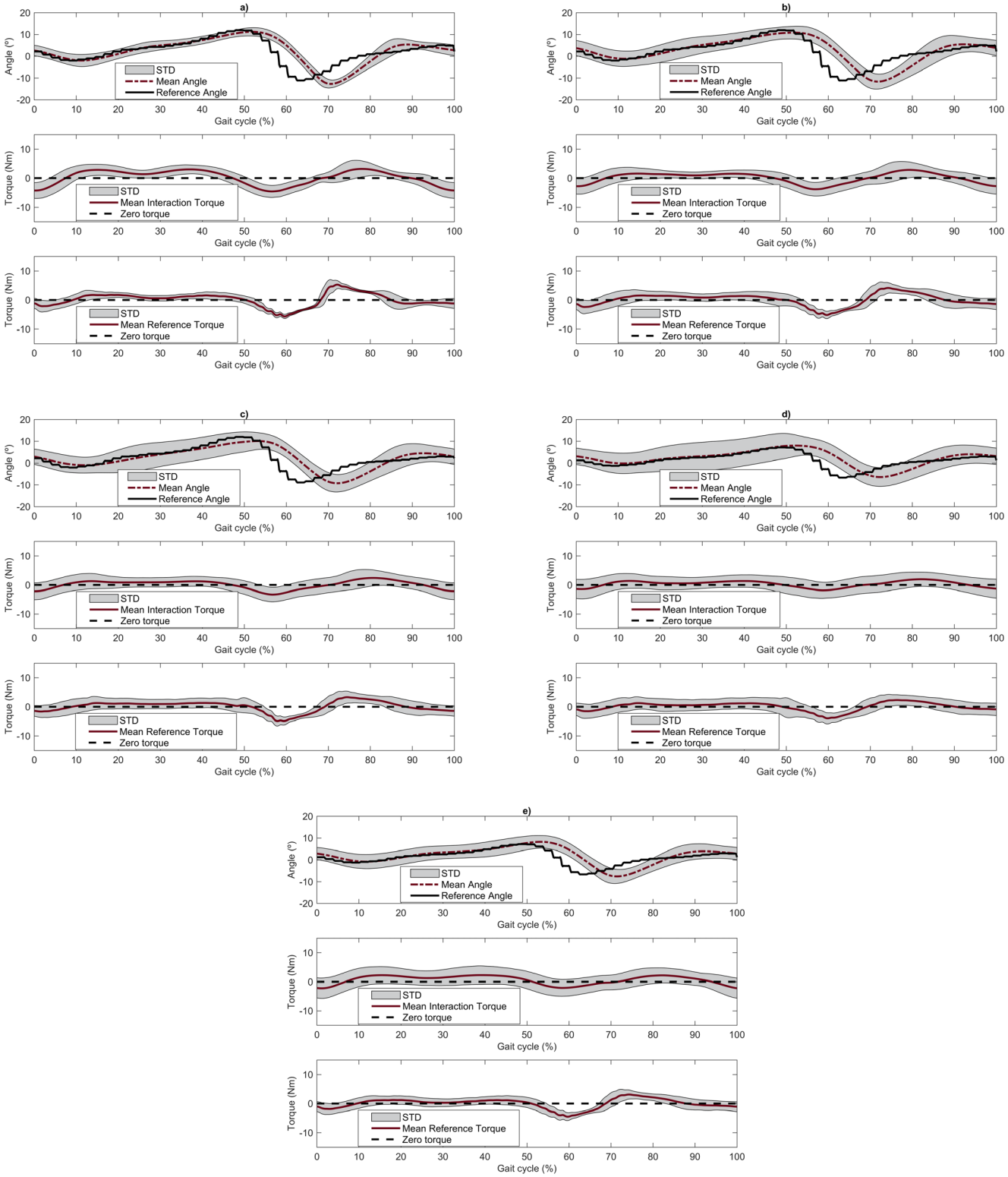

Fig. 6 Mean gait cycle walking at 1.0 km/h with the adaptive impedance control strategy considering: **a**) C_1, **b**) C_2, **c**) C_3, **d**) C_4, and **e**) C_5. In the graph representing angle, the mean angle and the corresponding standard-deviation, and the orthosis reference trajectory are presented. In the graphs representing torque, the mean human-orthosis interaction torque, the reference torque, and the corresponding standard-deviations are presented. Additionally, the zero torque is presented as the dashed black line

and the difference between gait speeds is more evident when lower values of the orthosis' reference trajectory were set (C_3 and C_4). From $C_1 \rightarrow C_2$, the interaction stiffness variation promoted a RMSE augmentation that is due to the users'

interaction with the orthotic device. Regarding the transition $C_4 \rightarrow C_5$, the error's dispersion decreased, as it was expected from Fig. 6, due to the increment in the interaction stiffness such that the orthosis imposed more its reference trajectory. The higher resulting assistive torque led to the lower RMSE.

In conclusion, from the results of Figs. 6 and 7, we can notice that the adaptive impedance control with adaptive gait trajectories successfully guided the users regarding the orthosis' reference trajectory, when high values of interaction stiffness are set, and promoted more freedom to the users' motion when low values of interaction stiffness are introduced. Therefore, the orthosis successfully created the effect of compliance/resistance. Regarding trajectory modifications, the users follow, in average, the orthosis' reference trajectory but, if required, the orthosis was compliant to deviations that were proportional to their active participation. By adapting the interaction stiffness and the gait trajectories per gait phase, the orthosis allows for the creation of intensity-adapted rehabilitation programs according to the users' needs and disability level, approaching a multi-functional assistive device.

Additionally, we verified that the adaptive impedance control strategy presented some delay regarding the orthosis' reference trajectory, which is discretized in Table 5 per condition and gait speed. The results indicate that there are no statistically significant differences in the assistance delay variation between the studied conditions (p value ≥ 0.05). This result indicates that these variations were not produced by the changes on the interaction stiffness and the orthosis' reference angle. The variations may be explained by the different interaction forces that each user applied to the orthotic device. Nonetheless, we verified that the delay increases with the gait speed, and this variation is, in general, considered statistically significant (p value $\leq 1.7 \times 10^{-2}$ for C_1, C_2, and C_4). The slower response for higher speeds may be caused by the orthosis' inherent mechanical features. In comparison with a pure trajectory control, the adaptive impedance control improved the control's delay in more than 10% considering both gait speeds (delay $\approx$ 250 ms for trajectory tracking control [22, 33]), which indicates that human-robot interaction yield more time-efficient assistance.

4.2 Biomechanical Effects Analysis

To assess the effects of changing the interaction stiffness and the orthosis' reference trajectory, we conducted a biomechanical analysis by evaluating the variation of the temporal, angular and muscular metrics between consecutive conditions for the assisted leg. A ratio between the muscular activation of the assisted leg and the non-assisted leg was also evaluated to assess the users' participation and to evaluate the hypothesis under study that this strategy fosters muscle strengthening.

4.2.1 Muscular Analysis

Figure 8 illustrates the mean muscular activity segmented per gait cycle for the *tibialis anterior* (TA) and *gastrocnemius lateralis* (GL) muscles for both assisted and non-assisted lower limbs at 1.0 km/h. The mean muscular activity observed at 1.6 km/h presents a similar pattern to the one illustrated in Fig. 8.

In general, we observed some variations on the muscular activity of assisted lower limb between consecutive conditions, and particularly on the GL muscle during the HO $\rightarrow$ TO phase. Nonetheless, the mean value ($\approx$ 9.5% and 12% of MVC, for 1.0 and 1.6 km/h, considering the TA, and $\approx$ 17.5% and 19.5% of MVC, for 1.0 and 1.6 km/h, considering GL) remained similar for all conditions, supported by the statistical analysis that indicates no significant differences (p value $\geq 6.3 \times 10^{-2}$ considering both 1.0 and 1.6 km/h, see Table 7). Although the differences were not considered statistically different, i.e., the mean muscular activity remained practically unaffected for both muscles between consecutive conditions, the participants reported an increased effort. This effort might have been accomplished by the internal muscles responsible for the gait, not producing significant changes in the superficial muscles' activation, as the TA and GL. Moreover, the

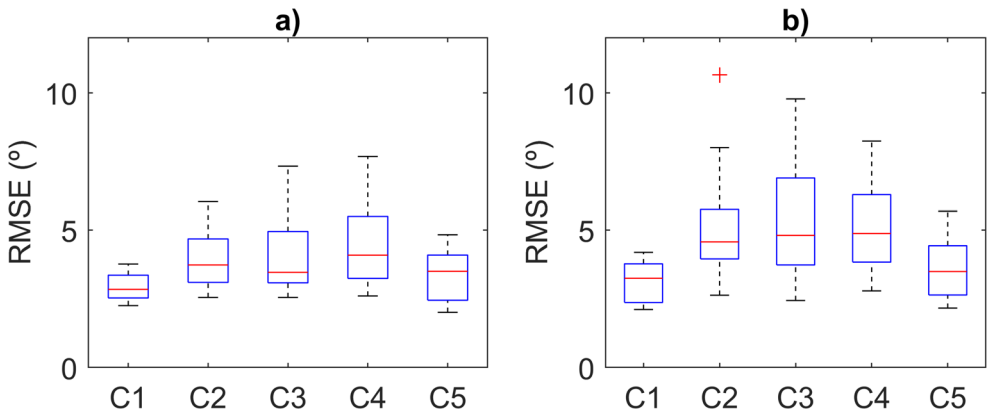

Fig. 7 RMSE dispersion for the five conditions, considering: **a**) 1.0 km/h and **b**) 1.6 km/h

Table 5 Strategy's delay (in ms) discretized by gait speed and condition. The mean value is represented at bold and the respective standard-deviation within parentheses

Condition	Gait Speed (km/h)	
	1.0	1.6
C_1	**163** (28.7)	**197** (32.1)
C_2	**179** (54.7)	**218** (46.1)
C_3	**182** (61.2)	**213** (52.3)
C_4	**169** (77.9)	**218** (65.2)
C_5	**187** (52.7)	**185** (27.1)

participants, as healthy subjects, may be able to compensate these changes over time more easily without producing significant changes in muscular activity.

By comparing both lower limbs, a more intense muscular activity is observed for the assisted leg for all conditions, with emphasis on the GL muscle. Figure 8 shows that robotics-based assistance maintains the healthy pattern reported on [34], however with greater magnitude for the assisted leg. This supports our hypothesis that this strategy entails a muscle reinforcement on the assisted lower limb that, in a rehabilitation context, is beneficial for users in the long-term to improve their muscular strength towards effective recovery. Even so, this strategy should be used after an intensive training with the orthotic device under a position control, so that users improve their gait pattern and recover some residual force to help them move the device. By Fig. 8, we also verified a slight deviation on the maximum muscular activation, with special emphasis on the GL muscle. This may be caused by some minimal misalignment between the user's limb and the orthotic device that may occur during walking. Although minimal, this is being considered by designing a user-tailored calf structure that will prevent this issue.

To assess the level of muscles' reinforcement, Table 6 presents the ratio between the muscular activity of the assisted leg vs non-assisted leg.

By analysing Table 6, we observed a higher muscular activity on the assisted GL muscle, which is responsible for the plantarflexion movement (propel the foot backward in the HO → TO phase), for both gait speeds since the ratio is always above 1. This result is in accordance with the results of Table 2, where it was found a higher interaction with the orthotic device for the HO → TO phase when the subjects walked in a passive mode of assistance. It is on this particular phase that the higher muscular activity is observed in healthy gait [34]. The orthosis, by appealing to the users' active participation, promotes muscle strengthening. This may be beneficial for post-stroke survivors since they usually exhibit muscle weakness at this phase. Regarding the TA muscle, the ratio between the assisted leg vs non-assisted leg is closer to 1 for both gait speeds, although slightly above for 1.6 km/h. The users use this muscle mainly for the dorsiflexion movement, namely during stance and during mid-swing to perform a new heel-strike. During mid-swing, the TA muscle is important to defeat gravity and perform the next heel-strike correctly. Figure 8 shows a higher muscular activation during this phase for the assisted TA muscle which might be beneficial for post-stroke survivors' presenting drop foot as it is their most weakened muscles. By using this strategy, the users are encouraged to actively participate in the rehabilitation therapy, enhancing their muscular activity which is relevant for long-term functional motor recovery.

4.2.2 Human-Orthosis Interaction Torque

Although the muscular activity of the assisted lower limb was not statistically different between consecutive conditions, the same finding was not observed for the human-orthosis interaction torque. Figure 9 indicates that the AAN impedance strategy allowed for variations on the interaction that each participant was performing with the orthotic device. This variation was more pronounced for the transitions where the interaction stiffness was modified and the orthosis gait trajectory was placed to 60% for all phases, i.e. in $C_4 \rightarrow C_5$ (especially for 1.0 km/h).

Figure 9 shows that changes in the interaction stiffness have modified the human-orthosis interaction torque dispersion. The interaction torque decreased from $C_1 \rightarrow C_2$, in which low values of interaction stiffness were set, and remained similar during $C_2 \rightarrow C_3$ and $C_3 \rightarrow C_4$, when the orthosis' reference trajectory was changed. The human-orthosis interaction torque increased again in $C_4 \rightarrow C_5$, in which high values of interaction stiffness were set. This might indicate that, for the healthy participants, a decrease on the interaction stiffness promotes a decrease in the human-orthosis interaction torque, while an increase of the values of interaction stiffness has the opposite effect.

The interaction torque may have a dual meaning depending on the values of interaction stiffness. With high values of interaction stiffness ($K = 1$), the strategy gives more power to the orthosis while the users' motion intention will not be so pronounced. In this case, the orthosis presents a more rigid behaviour and, consequently, the healthy participants tend to opposite more the orthosis motion, resulting in a higher interaction torque. On the other side, for lower values of interaction stiffness ($K \neq 1$), the orthosis acts more compliantly and, thus, the users' motion intention will be more evident. As they have more freedom to perform their preferred gait trajectory, the interaction torque may decrease since the orthosis moves according to their participation.

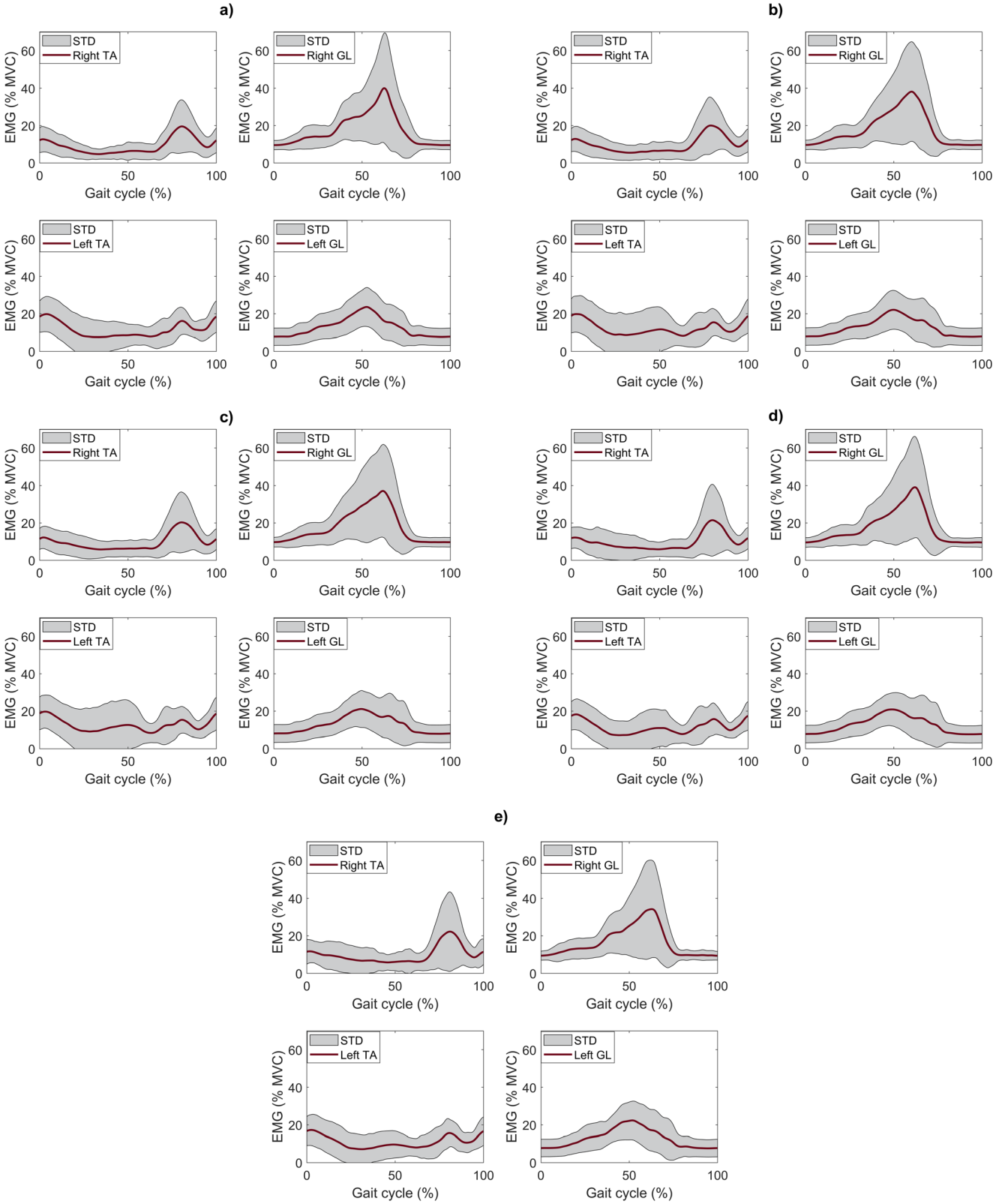

Fig. 8 Muscular activation for the *tibialis anterior* (left) and *gastrocnemius lateralis* (right) muscles regarding the assisted leg (above) and non-assisted leg (below) walking at 1.0 km/h, considering: **a**) C_1, **b**) C_2, **c**) C_3, **d**) C_4, and **e**) C_5

Table 6 Ratio of muscular activity for the five conditions. Mean is represented at bold and the standard-deviation within parentheses

Condition	*Tibialis anterior*		*Gastrocnemius lateralis*	
	1.0 km/h	1.6 km/h	1.0 km/h	1.6 km/h
C_1	**0.88** (0.38)	**1.01** (0.49)	**1.31** (0.52)	**1.14** (0.39)
C_2	**0.91** (0.42)	**0.99** (0.52)	**1.32** (0.53)	**1.15** (0.37)
C_3	**0.93** (0.46)	**1.08** (0.60)	**1.32** (0.53)	**1.15** (0.39)
C_4	**0.95** (0.47)	**1.09** (0.66)	**1.30** (0.55)	**1.14** (0.40)
C_5	**0.99** (0.49)	**1.11** (0.67)	**1.28** (0.57)	**1.17** (0.43)

This conclusion suggests that C_1 is not the most appropriated for subjects while walking at 1.0 km/h, since a statistically significant difference in the mean value of the human-orthosis interaction torque is observable during $C_1 \rightarrow C_2$ (p value $= 2 \times 10^{-3}$). During $C_2 \rightarrow C_3$ and $C_3 \rightarrow C_4$, the mean value of interaction torque remained practically unaffected. However, it increased significantly during $C_4 \rightarrow C_5$, when the orthosis become stiffer and imposed more its reference trajectory. With these results, we may conclude that users prefer a trajectory below the 100% of C_1 and above the 60% of C_5. This finding highlights the relevance of using adaptive trajectories. For 1.6 km/h, the change in the mean value of the human-orthosis interaction torque was only statistically significant when the trajectory was placed to the minimum (C_5) and the orthosis behaviour was stiffer (p value $= 1 \times 10^{-3}$). Therefore, we may conclude that subjects may prefer trajectories above the 60% of healthy gait pattern while walking at 1.6 km/h.

4.2.3 Angular Analysis

Figure 10 presents the percentual variation of the ankle angular metrics (maximum and minimum angles and ROM) for the assisted leg between consecutive conditions. We observed that the modification applied in $C_3 \rightarrow C_4$, where the entire trajectory was reduced to 60% of the healthy pattern, yielded a statistically significant reduction in the maximum ankle angle for both gait speeds (p value $= 1.3 \times 10^{-2}$ and 2.4×10^{-2} for 1.0 and 1.6 km/h, respectively). Additionally, the results suggest that the decreased interaction stiffness performed in the $C_4 \rightarrow C_5$ transition significantly reduced the maximum ankle angle (p value $\leq 6 \times 10^{-3}$ for both gait speeds).

Regarding the minimum ankle angle, the highest variations occurred when the orthosis' reference trajectory was modified, presenting a statistically significant difference in the transition $C_2 \rightarrow C_3$ (p value $\leq 1.7 \times 10^{-2}$ considering both gait speeds) and $C_3 \rightarrow C_4$ (p value $= 6 \times 10^{-3}$ for 1.0 km/h). The changes in the interaction stiffness entailed a statistically significant difference in the ankle's minimum trajectory during $C_4 \rightarrow C_5$ but only for 1.6 km/h (p value $= 1.2 \times 10^{-2}$). This result suggests that users may prefer a higher absolute value of minimum angle trajectory at 1.6 km/h. For 1.0 km/h, the variation was not significant which indicates that the users performed a similar minimum angle regarding the last condition.

The ROM decreased between consecutive conditions presenting a statistically significant decrease for $C_2 \rightarrow C_3$ (p value $\leq 3 \times 10^{-2}$ for both gait speeds), $C_3 \rightarrow C_4$ (p value $= 1 \times 10^{-3}$ for 1.0 km/h), and $C_4 \rightarrow C_5$ (p value $\leq 1.2 \times 10^{-2}$ for both gait speeds). Analysing Fig. 10, the variations of ROM decrease gradually for 1.0 km/h and were not so pronounced for 1.6 km/h until C_4. This highlights the previous conclusion that users may prefer higher trajectories as the gait speed increases. Therefore, we conclude that the gait trajectories modification is relevant to tackle the users' needs. Moreover, the adaptation per gait phase might be useful to address different gait pathologies that exhibit a deficit in specific gait phases. This will allow the creation of rehabilitation programs that enhance the users' functional motor recovery.

Regarding the knee articulation, the analysis was focused on the ROM variation (illustrated in Fig.11) since most of the angular variations were observed in the swing phase.

Figure 11 shows that the ROM variation between consecutive conditions is practically null, rounding 0%, which

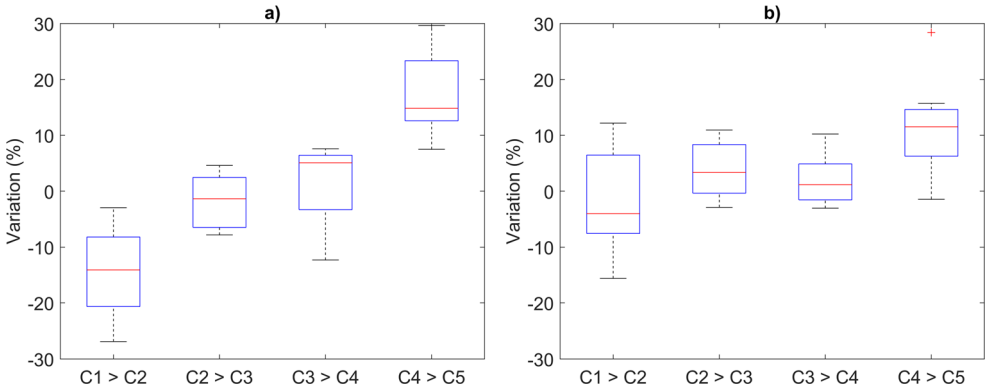

Fig. 9 Human-orthosis interaction torque variation between transitions and considering **a**) 1.0 km/h and **b**) 1.6 km/h

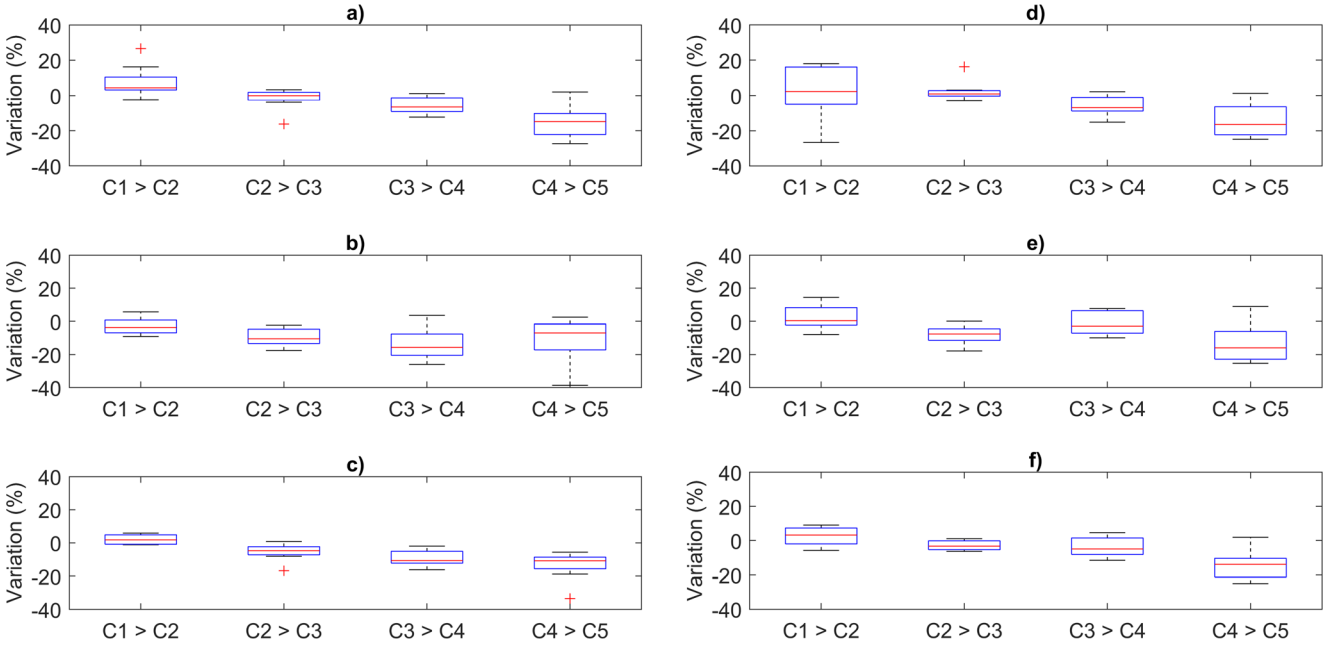

Fig. 10 Ankle angular variation considering the maximum value – **a**) for 1.0 km/h and **d**) for 1.6 km/h, the minimum value – **b**) for 1.0 km/h and **e)** for 1.6 km/h, and the range-of-motion – **c**) for 1.0 km/h and **f**) for 1.6 km/h

suggests that the modifications on the ankle assistance did not compromise the knee articulation. Moreover, the statistical tests supported this finding, revealing no statistically significant differences (p value ≥ 0.18 and ≥ 0.16 for 1.0 and 1.6 km/h, respectively) for the knee ROM. Findings pointed out that changing the interaction stiffness and the orthosis' reference trajectory did not result in compensatory motions at the knee joint, which is a beneficial result for clinical use of the proposed strategy.

4.2.4 Temporal Analysis

Figure 12 illustrates the variation of the temporal metrics (stance, swing, step, and stride time) between consecutive conditions and both studied gait speeds.

By analysing Fig. 12, we verified a slight variation on the stance and swing times that do not overcome an absolute variation of 10%. The results may suggest the existence of punctual fluctuations on the stance and swing times that, together, do not affect the stride time among conditions, which would be plausible since the gait speed is controlled by the treadmill. The step time also presented some fluctuations among conditions, similarly to the stance variation, which would be expected for healthy gait.

From the statistical analysis, there is not a direct relationship between the variations in gait temporal parameters and the adaptations in the interaction stiffness and orthosis' reference trajectory. The statistical analysis (see Table 7) supported this finding, revealing that the differences were not statistically significant (p value ≥ 0.11 and ≥ 0.21 for 1.0 and 1.6 km/h, respectively). This result would be expected since no temporal

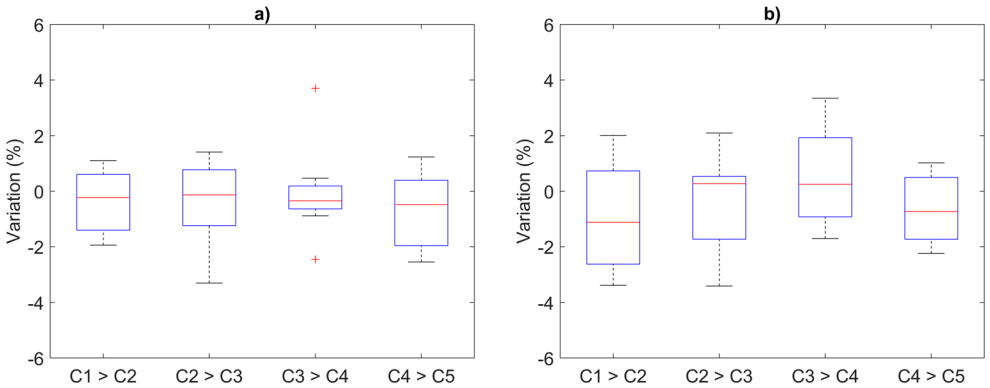

Fig. 11 Knee range-of-motion variation considering: **a**) 1.0 km/h and **b**) 1.6 km/h

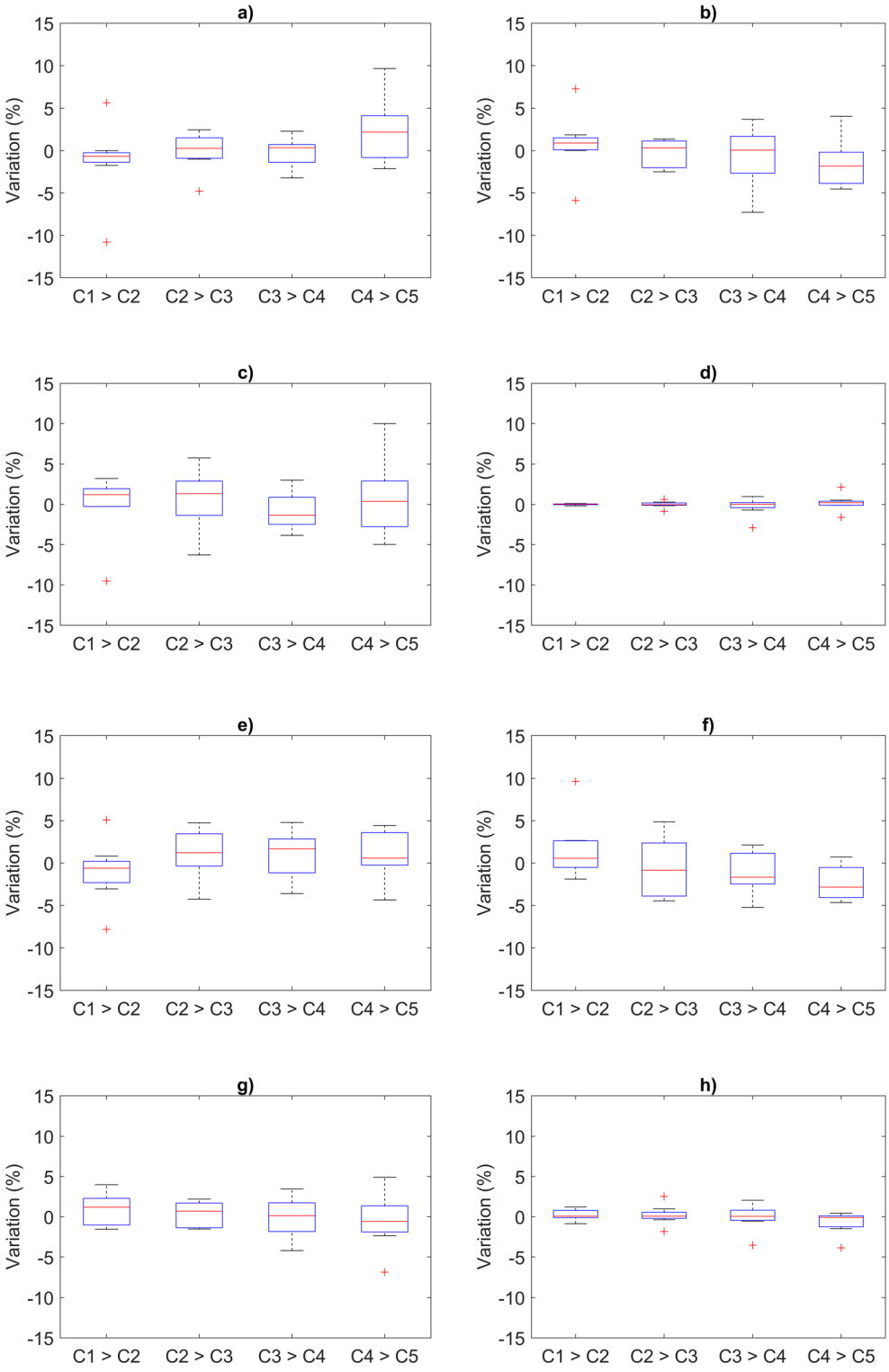

Fig. 12 Temporal variation for the stance time – **a**) and **e**); swing time – **b**) and **f**); step time – **c**) and **g**); and stride time – **d**) and **h**); considering 1.0 km/h and 1.6 km/h, respectively

aspects were modified between conditions. This finding indicates a positive effect of the proposed strategy that enables a more user-tailored assistance while ensuring that the orthosis can guide the end-user around a healthy gait pattern.

4.3 Qualitative Analysis

A qualitative analysis was conducted to assess the users' perceptions regarding the assistive strategy. The users were

instructed to answer eight questions (see Table 4) and leave a comment regarding their experience with the orthotic device. The questionnaire was performed after the experimental procedure, aiming not to influence the user's perception. Nevertheless, all participants were encouraged, at the beginning of the experimental procedure, to comment on their perception throughout the trials. Figure 13 presents the users' perception of some of the questions listed in Table 4.

Considering the users' perception, 63% of the participants agree that the strategy was able to guide them during the walking procedure. This result follows the conclusions raised in Fig. 6. However, some users reported some desynchronization with the orthotic device due to the lack of training. This issue might be solved by using biofeedback system to complement robotic-based gait training [35].

Regarding the fourth question, all users were able to verify when the system changed its behaviour by modifying the gait trajectory and/or the interaction stiffness (75% agree and 25% strongly agree). Nevertheless, there is no consensus if these changes give more freedom to walk since 38% agree, 25% are neutral, and 37% disagree. The result of this question can be interconnected with the effect of compliance/resistance that users felt while they are walking. From the results of Figs. 6 and 7, the dispersion that is observable for conditions when the interaction stiffness takes lower values proves that this strategy can modulate the orthosis' response to account the users' wills (if maintaining a healthy pattern). However, as the interaction stiffness is decreased or the gait trajectory is modified for lower values, the assistive torque the orthosis is giving will also be lesser. This could have two interpretations in the users' perspective. The users may feel the system compliant after the modifications, namely on C_2, C_3, and C_4, in a way that the system is allowing more deviations regarding the reference gait trajectory, creating a virtual tunnel. On the other hand, these changes can induce higher inertia to the movement since the orthosis is becoming progressively passive and, consequently, can be interpreted by the users as a higher effort training.

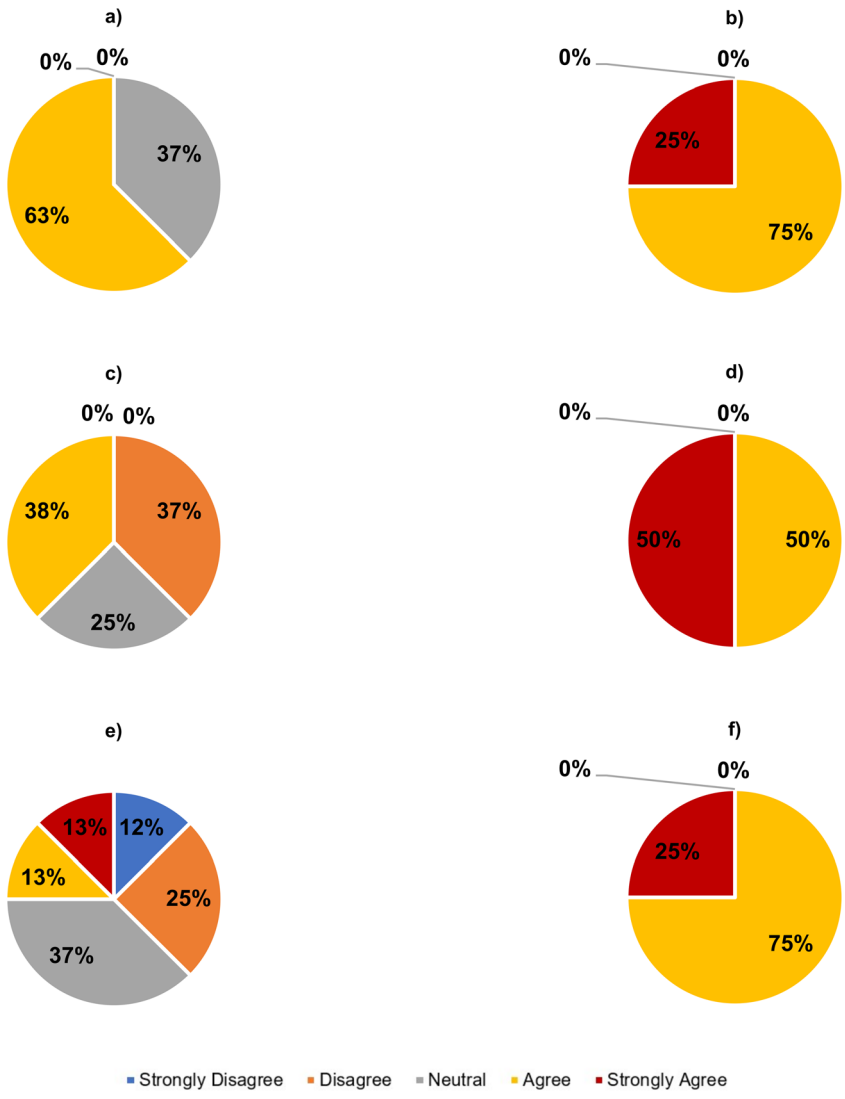

Fig. 13 Users' perception regarding the adaptive impedance control strategy considering: **a** question 2, **b** question 4, **c** question 5, **d** question 6, **e** question 7, and **f** question 8

Regarding the effort the users felt during the walking procedure, all of them felt that the changes in interaction stiffness or trajectory encouraged them to apply more effort during walking (50% agree and 50% strongly agree). The statistical results showed no significant differences in the average muscular activation. However, in comparison with the non-assisted leg, the muscular activity of the assisted leg was much higher. This explains the effort the users felt while walking with the orthotic device and follows the line of thought of this strategy.

4.4 Related Work

Prior works on literature have shown prominent results by employing adaptive impedance controls. The study [8] implemented a first-order impedance control in which the joint's torque is modulated according two impedance parameters: i) the linear elastic coefficient (K) and ii) the linear viscous coefficient (B). The authors use the interaction torque to estimate the patients' muscle torque. The authors verified that for higher impedance magnitudes, the exoskeleton imposed more its reference trajectory. On the other hand, for lower impedance values, the exoskeleton did not assist the user and the angular variations were higher. LOPES' exoskeleton is another multi-segment device that yields an impedance strategy [9]. The authors also consider this strategy relevant in robotics-based gait training since a purely position-based control presents the liming factor of reducing the kinematic variability. The exoskeleton is impedance-controlled using Bowden-cable series-elastic actuators. The results showed that the impedance control allowed for a very stiff movement for high values of joint's stiffness, which the authors named "robot-in-charge", and a flexible movement for low values of joint's stiffness, which the authors named "patient-in-charge". Moreover, the authors reported a muscle strengthening when using the impedance-controlled exoskeleton. Hussain et al. [17] also presented a similar strategy for a orthosis that assists the knee and hip joints. The orthosis also allows for two modes of operation. The authors found that this strategy allowed an increase on the users' participation when low assistance is given by the orthosis. These results are in line with those we found with our impedance-controlled orthosis. In [18, 19], the authors estimated the user's musculoskeletal torque and implemented a first-order impedance control by modulating the stiffness and damping parameters of the joint. The authors found this strategy is effective in estimating the patient's torque and effectively modulates the robot's assistance according to the user's participation. In [20, 21], the authors presented an assistive-resistive strategy to estimate the user's participation and adapt the robotic assistance accordingly. They found that adapting the impedance parameters allowed a more kinematic variability, whose results are in line with our work. Our work extends over these by estimating the interaction-based stiffness per gait phase and speed, considering the human-robot interaction torque and the real ankle trajectory. By adapting the interaction stiffness per gait phase, it allows for more meticulous adaptations instead of an isolated adaptation considering the whole gait cycle. Moreover, the gait trajectories modifications per gait phase in real-time allows for varying the assistance to fulfil the users' needs and enables to address the rehabilitation of various gait pathologies in the future. Additionally, our study complements the biomechanical assessment issued in previous studies [8, 9, 17–21] with a muscular activity study when both the interaction stiffness and the ankle's trajectory are changed in the impedance-controlled orthosis to assess its relevance for the rehabilitation of motor disabilities.

4.5 Limitations and Future Perspectives

The main limitation of our work is the lack of pathological participants to assess the biomechanical effects of using this strategy as a rehabilitation therapy. As a future perspective, we aim to design a longitudinal study and perform a rehabilitation program with persons suffering from a gait disability to perform the clinical validation of our orthosis and this strategy. A more extensive questionnaire will be issued, studying the users' perception throughout therapy. Future research insights also include the adaptation of both stiffness and damping coefficients and study their biomechanical effects by involving patients with motor disabilities. Further, we will automatically adapt both trajectory and interaction stiffness per gait phase considering the Human-in-loop to attain a more effective assist-as-needed therapy, while also attending for the clinicians' feedback.

5 Conclusion

This work presents and validates an assist-as-needed, adaptive impedance control strategy that can modulate the orthosis behaviour by innovatively change the human-robot interaction stiffness and the orthosis' reference trajectory per gait phase. The strategy successfully guides the users on a healthy gait pattern that may be adapted to fulfil their needs. Findings shows that users prefer different gait trajectories depending on the gait speed, highlighting the need for adapting gait trajectories. Further, the strategy can successfully pass from a passive assistance mode (the compliant mode), where the users have an active walking, to a more active mode of assistance (the stiff mode), where the orthosis imposes more its reference trajectory, approaching a multi-functional strategy. The users have more freedom to impose their preferred gait pattern when lower values of interaction stiffness are set. The quantitative and qualitative findings show that this strategy encourages the users to actively participate in the rehabilitation therapy, resulting in higher muscular activity, and that

they felt the effect of compliance/resistance that this strategy entails, cooperating with the orthotic device accordantly (human-robot cooperation). Moreover, we verified that this strategy did not entailed angular compensations on the knee ROM when the assistance was modified. Overall results support that this strategy may be applied for user-oriented and intensity-adapted gait training with different levels for personalization.

Appendix

Table 7 Level of significance (p value) for the biomechanical and muscular metrics considering 1.0 and 1.6 km/h. * means the result is statistically significant considering a level of confidence of 95% ($\alpha = 0.05$)

Condition	Temporal metrics								Muscular metrics				Interaction torque metrics	
	1.0 km/h				1.6 km/h				1.0 km/h		1.6 km/h		1.0 km/h	1.6 km/h
	Stance	Swing	Step	Stride	Stance	Swing	Step	Stride	Mean		Mean		Mean	Mean
									TA	GL	TA	GL		
$C_1 \rightarrow C_2$	0.46	0.49	0.97	0.30	0.34	0.27	0.21	0.35	6.3×10^{-2}	0.86	0.77	0.21	$2.0\times10^{-3*}$	0.84
$C_2 \rightarrow C_3$	0.86	0.75	0.47	0.86	0.37	0.69	0.67	0.66	0.74	0.85	0.12	0.61	0.58	6.7×10^{-2}
$C_3 \rightarrow C_4$	0.87	0.69	0.44	0.51	0.43	0.36	1.0	0.87	0.46	0.79	0.51	0.73	0.53	0.37
$C_4 \rightarrow C_5$	0.11	0.14	0.86	0.64	0.44	$2.1\times10^{-2*}$	0.67	0.24	0.29	0.17	0.26	0.33	0^{*}	$1.0\times10^{-3*}$
	Angular metrics													
	Ankle							Knee						
	1.0 km/h			1.6 km/h				1.0 km/h			1.6 km/h			
	Min	ROM	Max	Min	ROM	Max		ROM			ROM			
$C_1 \rightarrow C_2$	0.26	8.7×10^{-2}	$4.2\times10^{-2*}$	0.48	0.19	0.54		0.36			0.22			
$C_2 \rightarrow C_3$	$1.2\times10^{-2*}$	$2.5\times10^{-2*}$	0.46	$1.7\times10^{-2*}$	$3.0\times10^{-2*}$	0.22		0.47			0.56			
$C_3 \rightarrow C_4$	$6.0\times10^{-3*}$	$1.0\times10^{-3*}$	$1.3\times10^{-2*}$	0.67	0.13	$2.4\times10^{-2*}$		0.98			0.40			
$C_4 \rightarrow C_5$	0.10	$1.2\times10^{-2*}$	$4.0\times10^{-3*}$	$1.2\times10^{-2*}$	$3.0\times10^{-3*}$	$6.0\times10^{-3*}$		0.18			0.16			
	Control's delay													
	1.0 km/h							1.6 km/h						
$C_1 \rightarrow C_2$	5.1×10^{-2}							7.5×10^{-2}						
$C_2 \rightarrow C_3$	0.69							0.92						
$C_3 \rightarrow C_4$	0.38							0.93						
$C_4 \rightarrow C_5$	0.35							0.16						
	Control's delay between gait speeds													
C_1	0*													
C_2	$1.7\times10^{-2*}$													
C_3	0.12													
C_4	$9.0\times10^{-3*}$													
C_5	0.97													

Code Availability Not applicable.

Authors' Contributions **Conceptualization:** João M. Lopes, Joana Figueiredo, and Cristina P. Santos; **Data curation:** João M. Lopes and Cristiana Pinheiro; **Formal analysis:** João M. Lopes, Joana Figueiredo and Cristiana Pinheiro; **Funding acquisition:** Cristina P. Santos and Luís P. Reis; **Investigation:** João M. Lopes, Joana Figueiredo, and Cristiana Pinheiro; **Methodology:** João M. Lopes, Joana Figueiredo, and Cristina P. Santos; **Project administration**: Cristina P. Santos; **Resources:** Cristina P. Santos; **Software:** João M. Lopes; **Supervision:** Joana Figueiredo and Cristina P. Santos; **Validation:** João M. Lopes and Joana Figueiredo; **Visualization:** João M. Lopes; **Writing – original draft:** João M. Lopes; **Writing – review & editing:** Joana Figueiredo, Luís P. Reis, and Cristina P. Santos. All authors read and approved the final manuscript.

Funding This work has been supported by the FEDER Funds through the Programa Operacional Regional do Norte and national funds from Fundação para a Ciência e Tecnologia with the SmartOs project under Grant NORTE-01-0145-FEDER-030386, and under the national support to R&D units grant through the reference project UIDB/04436/2020 and UIDP/04436/2020.

Data Availability Not applicable.

Declarations

Ethics Approval The study had the ethical approval of the Ethics Committee in Life and Health Sciences with the code reference CEICVS 006/2020.

Consent to Participate Informed consent was obtained from all individual participants included in the study.

Consent to Publication The authors have the Ethics Committee in Life and Health Sciences approval for publishing this paper.

Conflicts of Interest/Competing Interests The authors declare that they have no competing or conflict of interests.

References

1. Mikolajczyk, T., Ciobanu, I., Badea, D.I., Iliescu, A., Pizzamiglio, S., Schauer, T., Seel, T., Seiciu, P.L., Turner, D.L., Berteanu, M.: Advanced technology for gait rehabilitation: an overview. Adv. Mech. Eng. **10**, 1–19 (2018). https://doi.org/10.1177/1687814018783627
2. Meng, W., Liu, Q., Zhou, Z., Ai, Q., Sheng, B., Xie, S.S.: Recent development of mechanisms and control strategies for robot-assisted lower limb rehabilitation. Mechatronics. **31**, 132–145 (2015). https://doi.org/10.1016/j.mechatronics.2015.04.005
3. Sanz-Merodio, D., Cestari, M., Arevalo, J.C., Garcia, E.: Control motion approach of a lower limb orthosis to reduce energy consumption. Int. J. Adv. Robot. Syst. **9**, 232 (2012). https://doi.org/10.5772/51903
4. Sankai, Y.: HAL: Hybrid assistive limb based on cybernics. Springer Tracts Adv. Robot. **66**, 25–34 (2010). https://doi.org/10.1007/978-3-642-14743-2_3
5. Esquenazi, A., Talaty, M., Packel, A., Saulino, M.: The Rewalk powered exoskeleton to restore ambulatory function to individuals with thoracic-level motor-complete spinal cord injury. Am. J. Phys. Med. Rehabil. **91**, 911–921 (2012). https://doi.org/10.1097/PHM.0b013e318269d9a3
6. Quintero, H.A., Farris, R.J., Hartigan, C., Clesson, I., Goldfarb, M.: A powered lower limb orthosis for providing legged mobility in paraplegic individuals. Top Spinal Cord Inj. Rehabiliation. **17**, 25–33 (2012). https://doi.org/10.1310/sci1701-25.A
7. Neuhaus, P.D., Noorden, J.H., Craig, T.J., Torres, T., Kirschbaum, J., Pratt, J.E.: Design and evaluation of Mina: a robotic orthosis for paraplegics. IEEE Int. Conf. Rehabil. Robot. (2011). https://doi.org/10.1109/ICORR.2011.5975468
8. Riener, R., Lünenburger, L., Jezernik, S., Anderschitz, M., Colombo, G., Dietz, V.: Patient-cooperative strategies for robot-aided treadmill training: first experimental results. IEEE Trans. Neural Syst. Rehabil. Eng. **13**, 380–394 (2005). https://doi.org/10.1109/TNSRE.2005.848628
9. Fleerkotte, B.M., Koopman, B., Buurke, J.H., Van Asseldonk, E.H.F., Van Der Kooij, H., Rietman, J.S.: The effect of impedance-controlled robotic gait training on walking ability and quality in individuals with chronic incomplete spinal cord injury: An explorative study. J. Neuroeng. Rehabil. **11**, 1–15 (2014). https://doi.org/10.1186/1743-0003-11-26
10. Lewis, C.L., Ferris, D.P.: Invariant hip moment pattern while walking with a robotic hip exoskeleton. J. Biomech. **44**, 789–793 (2011). https://doi.org/10.1016/j.jbiomech.2011.01.030
11. Blaya, J.A., Herr, H.: Adaptive control of a variable-impedance ankle-foot orthosis to assist drop-foot gait. IEEE Trans. Neural Syst. Rehabil. Eng. **12**, 24–31 (2004). https://doi.org/10.1109/TNSRE.2003.823266
12. Kao, P.C., Lewis, C.L., Ferris, D.P.: Invariant ankle moment patterns when walking with and without a robotic ankle exoskeleton. J. Biomech. **43**, 203–209 (2010). https://doi.org/10.1016/j.jbiomech.2009.09.030
13. Winter, D.A.: Biomechanics and motor control of human movement. John Wiley & Sons, Inc., Hoboken, New Jersey (2009)
14. Perry, J.: Gait analysis: normal and pathological function. SLACK Incorporated, Thorofare, New Jersey (1992)
15. Figueiredo, J., Felix, P., Santos, C.P., Moreno, J.C.: Towards human-knee orthosis interaction based on adaptive impedance control through stiffness adjustment. In: 2017 international conference on rehabilitation robotics (ICORR). pp. 406–411. IEEE, London (2017)
16. Cao, J., Xie, S.Q., Das, R., Zhu, G.L.: Control strategies for effective robot assisted gait rehabilitation: the state of art and future prospects. (2014)
17. Hussain, S., Xie, S.Q., Jamwal, P.K.: Adaptive impedance control of a robotic orthosis for gait rehabilitation. IEEE Trans. Cybern. **43**, 1025–1034 (2013). https://doi.org/10.1109/TSMCB.2012.2222374
18. Dos Santos, W.M., Siqueira, A.A.G.: Optimal impedance control for robot-Aided rehabilitation of walking based on estimation of patient behavior. Proc. IEEE RAS EMBS Int. Conf. Biomed. Robot. Biomechatronics. 2016-July, 1023–1028 (2016). https://doi.org/10.1109/BIOROB.2016.7523765
19. dos Santos, W.M., Siqueira, A.A.G.: Optimal impedance via model predictive control for robot-aided rehabilitation. Control. Eng. Pract. **93**, 104177 (2019). https://doi.org/10.1016/j.conengprac.2019.104177
20. Perez-Ibarra, J.C., Siqueira, A.A.G., Krebs, H.I.: Assist-As-needed ankle rehabilitation based on adaptive impedance control. IEEE Int. Conf. Rehabil. Robot. 2015-Septe, 723–728 (2015). https://doi.org/10.1109/ICORR.2015.7281287
21. Pérez-Ibarra, J.C., Siqueira, A.A.G., Silva-Couto, M.A., De Russo, T.L., Krebs, H.I.: Adaptive impedance control applied to robot-aided neuro-rehabilitation of the ankle. IEEE Robot. Autom. Lett. **4**, 185–192 (2019). https://doi.org/10.1109/LRA.2018.2885165
22. Lopes, J.M., Pinheiro, C., Figueiredo, J., Reis, L.P., Santos, C.P.: Assist-as-needed impedance control strategy for a wearable ankle robotic orthosis. In: IEEE International Conference on Autonomous Robot Systems and Competitions (ICARSC). pp. 10–15. , Ponta Delgada, Portugal (2020)
23. Tucker, M.R., Lambercy, O., Gassert, R., Olivier, J., Bleuler, H., Bouri, M., Pagel, A., Riener, R., Vallery, H., Del Millán, J.R.: Control strategies for active lower extremity prosthetics and orthotics: a review. J. Neuroeng. Rehabil. **12**, 1 (2015). https://doi.org/10.1186/1743-0003-12-1
24. Hogan, N.: Impedance control: an approach to manipulation. J. Dyn. Syst. Meas. Control. 1–24 (1985). https://doi.org/10.1115/1.3140702
25. Bortole, M.: Robotic Exoskeleton with an Assist-as-Needed Control Strategy for Gait Rehabilitation after Stroke, (2014)
26. Molugaram, K., Rao, G.S., Molugaram, K., Rao, G.S.: Chapter 5 – curve fitting. In: Statistical techniques for transportation engineering. pp. 281–292 (2017)
27. Figueiredo, J., Félix, P., Costa, L., Moreno, J.C., Santos, C.P.: Gait event detection in controlled and real-life situations: repeated measures from healthy subjects. IEEE Trans. Neural Syst. Rehabil. Eng. **26**, 1945–1956 (2018). https://doi.org/10.1109/TNSRE.2018.2868094
28. Al-Amri, M., Nicholas, K., Button, K., Sparkes, V., Sheeran, L., Davies, J.L.: Inertial measurement units for clinical movement analysis: reliability and concurrent validity. Sensors (Switzerland). **18**(1–29), (2018). https://doi.org/10.3390/s18030719
29. Poitras, I., Bielmann, M., Campeau-Lecours, A., Mercier, C., Bouyer, L.J., Roy, J.S.: Validity of wearable sensors at the shoulder joint: combining wireless electromyography sensors and inertial measurement units to perform physical workplace assessments. Sensors (Switzerland). **19**, (2019). https://doi.org/10.3390/s19081885
30. Hermens, H.J., Freriks, B., Disselhorst-Glug, C., Rau, G.: Development of recommendations for SEMG sensors and sensor placement procedures. J. Electromyogr. Kinesiol. 361–374 (2000). https://doi.org/10.1007/s10750-015-2551-3, 2018
31. Brooke, J.: SUS: A Quick and Dirty Usability Scale. In: Jordan, P., Thomas, B., Weerdmeester, B.A., and McClelland, I.L. (eds.) Usability evaluation in industry. pp. 189–194. Taylor & Francis Ltd (1996)
32. Sauro, J., Lewis, J.R.: Quantifying the user experience: practical statistics for user research. Elsevier. (2012)
33. Fernandes, P.N., Figueiredo, J., Moreno, J.C., Santos, C.P.: Feedback-error learning control for powered assistive devices. In:

MEDICON 2019: XV Mediterranean Conference on Medical and Biological Engineering and Computing. pp. 1998–2013 (2020)
34. Van Den Bogert, A.J., Geijtenbeek, T., Even-Zohar, O., Steenbrink, F., Hardin, E.C.: A real-time system for biomechanical analysis of human movement and muscle function. Med. Biol. Eng. Comput. **51**, 1069–1077 (2013). https://doi.org/10.1007/s11517-013-1076-z
35. Pinheiro, C., Lopes, J.M., Figueiredo, J., Goncalves, L.M., Santos, C.P.: Design and technical validation of a wearable biofeedback system for robotic gait rehabilitation. 2020 IEEE Int. Conf. Auton. Robot Syst. Compet. ICARSC. **2020**, 16–21 (2020). https://doi.org/10.1109/ICARSC49921.2020.9096105

João M. Lopes received the M.Sc. degree in Biomedical Engineering, specialized in Medical Electronics, in 2019, from the University of Minho, Portugal. He is currently a Ph.D. student in Biomedical Engineering at BiRDLab from the Center for MicroElectroMechanical Systems (CMEMS), also from University of Minho. He was a Research Fellow along with SmartOs project at CMEMS. He published 6 articles in conferences and participated in 5 events. He received 4 awards and/or honors. His research interests include assistive devices and control strategies towards personalized gait rehabilitation and assistance.

Joana Figueiredo received the M.Sc. degree in Biomedical Engineering, specialized in Medical Electronics, in 2015, and the Ph.D. degree in Biomedical Engineering in 2019 both from the University of Minho, Portugal, and in cooperation with the Neural Rehabilitation Group from Cajal Institute, Spain. She is a postdoctoral researcher in the SmartOs project at the Center for MicroElectroMechanical Systems (CMEMS) and a guest Assistant Professor at the University of Minho, Portugal. She supervised the scientific and technological work of 11 master students from different fields of engineering. She is the first author of 3 publications in scientific journals of the motor rehabilitation field and more than 20 ISI/Scopus conference publications. She is a Special Issue Editor of the journal Sensors. Her research interests include wearable assistive devices and motor control strategies towards personalized gait rehabilitation and assistance. Additionally, her research covers the development of AI strategies to analyze and predict human motion and human-robot interaction. Dr. Figueiredo's awards include the Jaime Filipe Award as Innovative Technology for Motor Rehabilitation in 2017, the IEEE International Conference on Autonomous Robot Systems and Competitions Best Paper Award in 2019, and co-advisor of the Fraunhofer Best Portuguese MSc Thesis in Biomedical Engineering in 2019.

Cristiana Pinheiro is a Ph.D. student in Biomedical Engineering at BiRDLab from the Centre of MicroElectroMechanical Systems (CMEMS), University of Minho, Portugal. She completed Integrated Master's Degree in Biomedical Engineering in 2019 by University of Minho. She has 7 conference papers published and 1 journal article. Participated in 8 events. Received 4 distinctions. She worked as a Visiting Researcher. Participated as a Research Fellow in 1 project. She works in Engineering Sciences and Technologies with an emphasis on Electrotechnical Engineering, Electronics, and Informatics with an emphasis on Robotics. The most frequent terms in the context of scientific and technological production are robotics, wearable biofeedback system, gait rehabilitation, wearable active orthosis, human-robot interaction, stroke, and user-centered design.

Luís P. Reis is an Associate Professor at the University of Porto in Portugal and Director of LIACC – Artificial Intelligence and Computer Science Laboratory where he also coordinates the Human-Machine Intelligent Cooperation Research Group. He is an IEEE Senior Member, and he was president of the Portuguese Society for Robotics, is vice-president of the Portuguese Association for Artificial Intelligence and was the director of MIEGSI. During the last 25 years, he has lectured courses, at the University, on Artificial Intelligence, Intelligent Robotics, Multi-Agent Systems, Simulation and Modelling, Games and Interaction, Educational/Serious Games and Computer Programming. He was the principal investigator of more than 10 research projects in those areas. He won more than 50 scientific awards including wining more than 15 RoboCup international competitions and best papers at conferences such as ICEIS, Robotica, IEEE ICARSC and ICAART. He supervised 21 PhD and 110 MSc theses to completion and is supervising 8 PhD theses. He evaluated more than 50 projects and proposals for FP6, FP7, Horizon2020, FCT and ANI. He was a plenary speaker of several international conferences such as ICAART, ICINCO, LARS/SBR, WAF, IcSports, SYROCO, CLAWAR, and WCQR. He organized more than 50 international scientific events and belonged to the Program Committee of more than 250 scientific events. He is the author of more than 350 publications in international conferences and journals (indexed at SCOPUS or ISI Web of Knowledge).

Cristina P. Santos graduated in Industrial Electronics Engineering in 1994, received the M.Sc. degree in 1998 and the Ph.D. degree in 2003, all from the University of Minho, Guimarães, Portugal. Her PhD thesis work was in cooperation with the Centre National de Recherche Scientific (CNRS–CNRC) Marseille, France. She is an Auxiliar Professor at the University of Minho, Industrial Electronics Department, Portugal. She was the principal investigator of more than 10 research projects in the areas of Robotics and Artificial Intelligence, particularly, locomotion field and rehabilitation. She is currently supervising 8 Ph.D. thesis and has supervised 40 MSc thesis to completion. She is the author of more than 100 publications in ISI and Scopus international conferences and journals. Her research focus on the extension of the use of the dynamical systems theory to the achievement of more complex behavior for robots: generate locomotion for multi-dof robots; achieve cooperativity among multi-robots and learning. Recently her research interests focus on methods to characterize human motion and designing robots and robot controllers for the rehabilitation of patients suffering from motor problems. Dr. Santos' awards include the Jaime Filipe Award in 2015, 2016, and 2017, co-author of the IEEE International Conference on Autonomous Robot Systems and Competitions Best Paper Award in 2019, and the advisor of the Fraunhofer Best Portuguese MSc Thesis in Biomedical Engineering in 2019.